

# 1 **Human cytomegalovirus strain diversity and dynamics reveal the** 2 **donor lung as a major contributor after transplantation**

3 Büsra Külekci<sup>1</sup>, Stefan Schwarz<sup>2</sup>, Nadja Brait<sup>3</sup>, Nicole Perkmann-Nagele<sup>4</sup>, Peter Jaksch<sup>2</sup>, Konrad  
4 Hoetzenecker<sup>2</sup>, Elisabeth Puchhammer-Stöckl<sup>1</sup>, Irene Goerzer<sup>1§</sup>

5 1 Center for Virology, Medical University of Vienna, Vienna, Austria

6 2 Department of Thoracic Surgery, Medical University of Vienna, Austria

7 3 Groningen Institute for Evolutionary Life Sciences, University of Groningen, Groningen,  
8 Netherlands

9 4 Division of Clinical Virology, Medical University of Vienna, Austria

10 § Corresponding author: E-mail: [irene.goerzer@meduniwien.ac.at](mailto:irene.goerzer@meduniwien.ac.at)

## 11 **Abstract**

12 Mixed human cytomegalovirus (HCMV) strain infections are frequent in lung transplant recipients  
13 (LTRs). To date, the influence of the donor (D) and recipient (R) HCMV-serostatus on intra-host  
14 HCMV strain composition and replication dynamics after transplantation is only poorly understood.

15 Here, we investigated ten pre-transplant lungs from HCMV-seropositive donors, and 163 sequential  
16 HCMV-DNA positive plasma and bronchoalveolar lavage samples from 50 LTRs with multiviremic  
17 episodes post-transplantation. The study cohort included D+R+ (38%), D+R- (36%), and D-R+ (26%)  
18 patients. All samples were subjected to quantitative genotyping by short amplicon deep sequencing,  
19 and 24 thereof were additionally PacBio long-read sequenced for genotype linkages.

20 We find that D+R+ patients show a significantly elevated intra-host strain diversity compared to D+R-  
21 and D-R+ patients ( $P=0.0089$ ). Both D+ patient groups display significantly higher replication  
22 dynamics than D- patients ( $P=0.0061$ ). Five out of ten pre-transplant donor lungs were HCMV-DNA  
23 positive, whereof in three multiple HCMV strains were detected, indicating that multi-strain

24 transmission via lung transplantation is likely. Using long reads, we show that intra-host haplotypes  
25 can share distinctly linked genotypes, which limits overall intra-host diversity in mixed infections.  
26 Together, our findings demonstrate donor-derived strains as a main source for increased HCMV strain  
27 diversity and dynamics post-transplantation, while a relatively limited number of intra-host strains  
28 may facilitate rapid adaptation to changing environments in the host. These results foster targeted  
29 strategies to mitigate the potential transmission of the donor strain reservoir with the allograft.

30

31 **Keywords:**

32 human cytomegalovirus, intra-host strain diversity, mixed infections, lung transplant, viral strain  
33 dynamics, PacBio sequencing

34

35

## 36 Introduction

37 Human cytomegalovirus (HCMV), a double-stranded DNA virus of the  $\beta$ -herpesvirus family,  
38 establishes a lifelong latent infection with reactivation episodes. Multiple HCMV strains (i.e. mixed  
39 infections) can be acquired during a person's lifetime (Meyer-König et al., 1998)(Puchhammer-Stöckl  
40 et al., 2006) and are specifically frequent in transplant patients, where HCMV strains can be donor- or  
41 recipient-derived (D/R) or both (Puchhammer-Stöckl & Görzer, 2011). While infections in healthy  
42 adults are typically asymptomatic, they can lead to severe outcomes in those with immature or  
43 compromised immune systems (Fulkerson et al., 2021). Multiple strains provide an opportunity for  
44 viral recombination, selection for antiviral drug-resistant mutants and might consequently impact viral  
45 pathogenicity (Renzette et al., 2014). In fact, HCMV-infection related increased morbidity and  
46 mortality remains a high risk for lung transplant recipients (LTRs) (Almaghrabi et al., 2017).

47 With about 236 kbp in size, HCMV consists of predominantly conserved regions across strains and  
48 some highly polymorphic hotspots spread across the genome (Renzette et al., 2014). These variable  
49 loci result in a limited number of distinct genotypes that have been extensively used to study  
50 population-level HCMV diversity found within and between hosts, primarily focusing on  
51 glycoproteins such as gB, gN, gO and gH (Wang et al., 2021). Various techniques, including  
52 restriction fragment length polymorphism (RLFP) analysis (Huang et al., 1980), targeted amplicon  
53 sequencing (Puchhammer-Stöckl et al., 2006)(Coaquette et al., 2004)(Sowmya & Madhavan,  
54 2009)(Hasing et al., 2021), and whole-genome sequencing (Dhingra et al., 2021)(Suárez et al., 2020)  
55 have been used. With increasing sequencing depth of next-generation sequencing platforms, the  
56 detection of low-frequency variants, i.e. minors became possible (Görzer et al., 2010). Currently, there  
57 is mounting evidence that HCMV exists as a heterogeneous collection of genomes with variations in  
58 composition and distribution between anatomical compartments (Renzette et al., 2013)(Hage et al.,  
59 2017) and over time (Dhingra et al., 2021)(Suárez et al., 2020)(Görzer et al., 2010)(Hage et al., 2017).  
60 However, in samples with mixed strains, determination of individual consensus sequences using short  
61 reads presents a challenge. In 2019, Cudini *et al.* introduced a computational method to reconstruct  
62 individual sequences within a sample from short-read data. They showed that the high nucleotide

63 diversity of HCMV samples is due to mixed infections (Cudini et al., 2019). Another possibility to  
64 determine individual sequences in a sample is by single-read sequencing of long reads. We recently  
65 demonstrated that the true diversity in mixed populations of patient samples can be underestimated by  
66 short-read sequencing, since haplotype sequences sharing long stretches of sequence identity even in  
67 amplicon target regions can be missed, highlighting the utility of long reads (Brait et al., 2022).

68 Despite extensive research on HCMV strain diversity, much less is known about strain dynamics in  
69 LTRs, which can harbour heterogeneous viral populations (Görzer et al., 2008). In principle, dynamics  
70 can change by introducing new strains to the population, by reactivation of latent strains, *de novo*  
71 mutation, recombination or through the change in relative frequencies of present strains. It has been  
72 shown that reinfection with donor strains and reactivations of recipient strains can occur similarly  
73 often, although this is difficult to distinguish in mixed infected patients (Manuel, Pang, et al., 2009).  
74 Also, multiple strain transmissions from the donor organ to the recipient and a shift in strain  
75 predominance over time were found to be common (Hasing et al., 2021)(Hage et al., 2017), suggesting  
76 a complex dynamic post-transplantation.

77 Here, we combine Illumina deep-sequence and PacBio long-read sequence data from 163 specimens  
78 of 50 LTRs of different D/R risk groups with recurrent HCMV infection, to examine within-patient  
79 HCMV strain diversity and dynamics. This retrospective study points out major contributors to viral  
80 diversity in transplant patients leading to increased dynamics post-transplantation.

81



## 82 Results

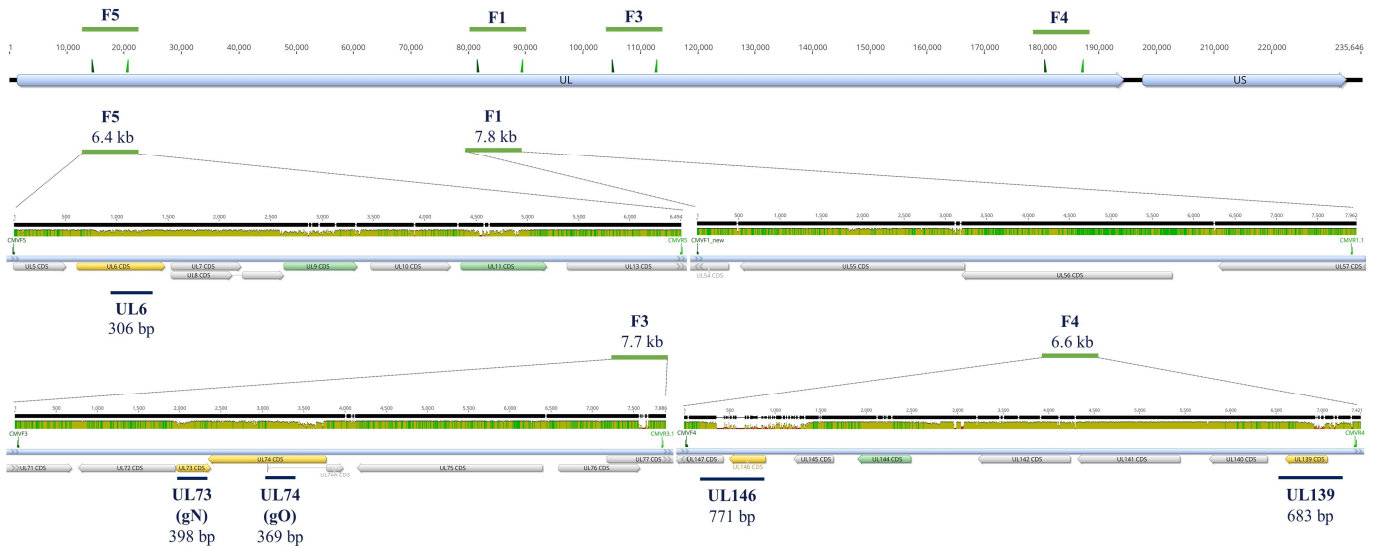
### 83 PCR genotyping success rates of five genomic regions and overall genotype distribution

84 For this study, 50 LTRs with at least two HCMV DNAemia episodes with  $>10^2$  copies/mL either in  
85 the bronchoalveolar lavage (BAL) or EDTA-plasma (EP) or both, and one sample with  $>10^3$   
86 copies/mL during the follow-up period of at least 185 days post-transplantation were included (details  
87 are provided in Materials and Methods). Genotypes of up to five polymorphic loci, namely UL6,  
88 UL73 (gN), UL74 (gO), UL139, UL146 (Figure 1) were assessed in 163 specimens consisting of 89  
89 BAL and 74 EP samples by Illumina deep sequencing as described previously (Brait et al., 2022). This  
90 resulted in genotyping success rates for the five loci ranging between 67% and 85% (Figure 2A).

91 Despite a comparable viral load distribution, BAL samples had a higher genotyping success rate for all  
92 loci than EP samples (Figure 2A). A detailed summary of PCR performances and the number of  
93 genotypes per locus are provided in Supplementary Table 1. We observed a trend towards higher viral  
94 loads with increasing numbers of maximally detected genotypes (Figure 2–figure supplement 1A).  
95 Considering the slightly different PCR genotyping success rates of the different loci, we also analysed  
96 each region separately (Figure 2–figure supplement 1B). Here, the association between higher viral  
97 loads and increasing genotype numbers was significant for gN ( $P = 0.0093$ ), UL6 ( $P = 0.0490$ ) and  
98 UL146 ( $P = 0.0031$ ) but not for gO and UL139. The samples with the highest genotype numbers ( $\geq 3$ )  
99 did not have the highest viral loads. Of all samples with  $\geq 2$  genotypes at any locus 79% (49 out of 62)  
100 showed a single genotype in one of the five regions. These data indicate that the applied genotyping  
101 PCRs are highly sensitive also for samples with low viral loads starting from  $10^2$  copies/mL, thus are  
102 well suitable for identifying mixed genotypes in clinical samples.

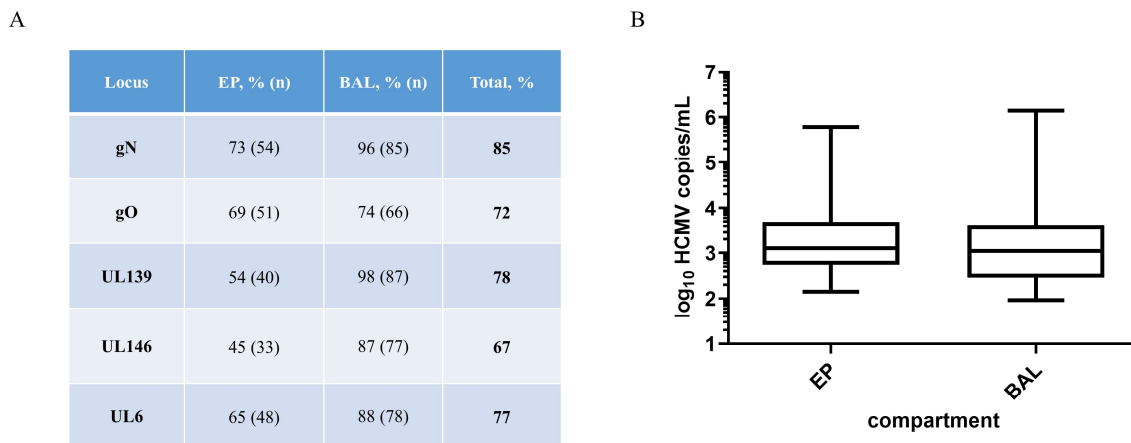
103 We detected each genotype of the five loci in one and up to 20 LTRs, except for UL146-3, UL146-5  
104 and UL146-6, which we did not find in any sample (Figure 2–figure supplement 2). Each genotype  
105 was also found as a major genotype (defined as  $>70\%$  of all reads) in at least one sample. No  
106 significant differences between genotypes and viral loads were found for any of the five loci and this is  
107 illustrated for gO in Figure 2–figure supplement 3. These findings suggest that none of the detected

108 genotypes had an obvious replication advantage over the others. The absence of UL146-3, UL146-5  
 109 and UL146-6, in contrast, may be indicative for functional differences among UL146 genotypes.  
 110



111 **Figure 1. Locations of amplicon target regions along the HCMV genome of strain Merlin (NCBI: AY446894).** The first track shows the overall HCMV genome structure that consists of a unique long (UL) and a unique short (US) region. Above, forward and reverse primers for the long amplicons (F5, F1, F3, F4) are depicted in dark and light green, respectively. Next, a zoom-in into these four long amplicons (green horizontal lines with amplicon sizes) are shown separately. The mean pairwise nucleotide identity for over 200 published sequences for these regions is shown in three colours: green (100%), brown ( $\geq 30\%$  -<100%), red ( $\leq 30\%$ ). Annotated coding sequences (CDS) are shown in grey boxes and those used for short-read and long-read genotyping are orange and green, respectively. Lastly, blue lines below each long amplicon indicate short amplicon regions (UL6, UL73, UL74, UL146 and UL139) and the respective amplicon sizes. Graphs were generated with geneious prime 2019.0.3.

112

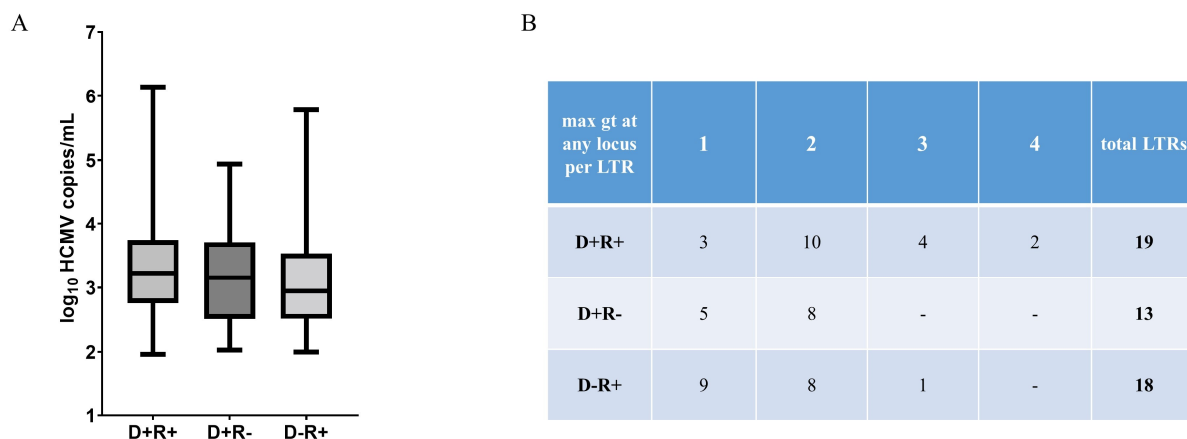


113 **Figure 2. Genotyping performances for the five regions gN (UL73), gO (UL74), UL139, UL146 and UL6 and the viral load distribution for EP and BAL samples.** A: Genotyping success in percent genotyped sample/total number of samples of this compartment. In total, gN has the highest PCR success rate and UL146 the lowest.  
 B: Box whisker plots of the viral load of EP and BAL samples of the total cohort. The viral load distribution is not different between sample types ( $P = 0.301$ ,  $n = 163$ , Mann-Whitney test).  
 EP, EDTA-Plasma; BAL, bronchoalveolar lavage

114

115 **Donor and recipient HCMV-seropositive patients display higher genotype diversity**

116 We aimed to analyse the genotype diversity among the three HCMV serostatus combination groups,  
 117 whereof 19 were D+R+ (38%), followed by 18 D-R+ (36%) and 13 D+R- LTR patients (26%).  
 118 Similar HCMV DNA loads were observed between all three D/R serostatus combinations (Figure 3A).  
 119 For each patient the maximum number of genotypes detected at any of the five loci and in any BAL  
 120 and EP sample was counted (Figure 3B). More than one genotype was found in 84% of D+R+ patients  
 121 compared to 62% and 50% in D+R- and D-R+ patients, respectively. D+R+ patients were significantly  
 122 more frequently infected with > 2 genotypes (6/19) than D+R- and D-R+ patients (1/31) ( $P = 0.0089$ ;  
 123 Fisher's exact test). Moreover, the D+R+ patient group shows the highest numbers of genotypes with  
 124 up to four genotypes in two LTRs (Figure 3B). These data suggest that both, lung donor and recipient  
 125 contribute to the HCMV strain diversity in D+R+ patients.



126

**Figure 3. Viral load and maximum number of genotypes (max gt) in lung transplant recipients (LTRs) with different HCMV serostatus combinations of donor (D) and recipient (R).**

**A:** No significant difference in viral load between the three HCMV serostatus combination groups is observed ( $P = 0.2626$ ,  $n = 163$ , Kruskal-Wallis test plus *post hoc* Dunn's multiple comparisons test)

**B:** The maximum number of genotypes (gt) at any of the five loci detected for each LTR is provided ( $n = 50$ ).

127

128 **Donor HCMV-seropositive patients exhibit higher genotype dynamics over time**

129 Next, we analysed how the genotype composition within a patient changes over time in the three  
 130 serostatus patient groups. In 36/50 LTRs genotyping data of at least two episodes of HCMV DNAemia  
 131 in the same compartment were available and allowed analysis of intra-host genotype dynamics over  
 132 time (Figure 4A). In total, 26 BAL and 14 EP sample pairs were analysed (Supplementary Table 2).  
 133 The median time difference between the paired samples was 179 days (range = 14 - 531 days). LTRs

134 with at least one sample with  $\geq 2$  genotypes at any loci or differing genotypes at different time points  
135 were defined as mixed infected ( $n = 27$ ). On the contrary, in single infected patients one genotype was  
136 identified longitudinally ( $n = 9$ ). We defined the total genotype dynamics over time as a change in two  
137 variables: 1) increase in genotype number and 2) change in relative genotype frequency. The former  
138 describes an increase in genotype number between time points 1 and 2, while the latter accounts for a  
139 predominance change in the major genotype (defined as  $>70\%$  of all reads) between the two episodes.

140 D+ patients showed significantly higher total dynamics than D- patients ( $P = 0.0061$ ) (Figure 4B, 4C)  
141 and a trend in the increase in genotype numbers ( $P = 0.0899$ ). In 69% of D+R+ patients a change in  
142 predominance was observed compared to 33% each in the other two patient groups. Antiviral  
143 medication, which may influence strain dynamics, was similarly frequent between single- and mixed-  
144 infected LTRs ( $P > 0.9999$ ,  $n = 34$ ), between mixed-infected D+ and D- LTRs ( $P = 0.1972$ ,  $n = 26$ ),  
145 and between LTRs with and without total dynamics ( $P > 0.9999$ ,  $n = 26$ ). These data indicate that  
146 there is no significant medication effect on strain dynamics.

A

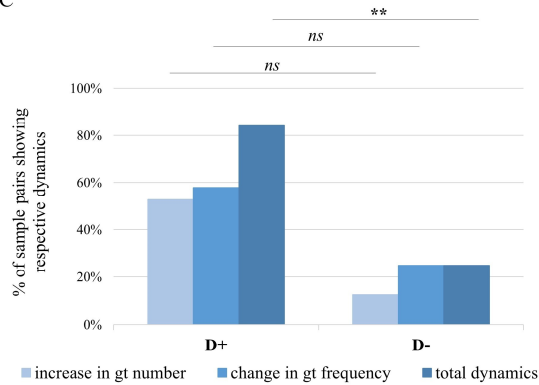
	mixed strain infected		single strain infected	
	LTRs	sample pairs	LTRs	sample pairs
D+R+	13	16	2	2
D+R-	6	6	4	4
D-R+	8	9	3	3
Total n	27	31	9	9

B

	increase in gt number	change in gt frequency	total dynamics	antiviral medication
D+R+	8/16	11/16	13/16	11/15 (1 nd*)
D+R-	4/6	2/6	5/6	5/6
D-R+	1/9	3/9	3/9	5/9

\* nd, not determined (clinical data not available)

C



147

#### Figure 4. Intra-host genotype dynamics over time in lung transplant recipients (LTRs) of the three HCMV-serostatus combination groups.

**A:** The numbers of LTRs and the number of sample pairs comprising the dynamics cohort are categorised into the three serostatus groups. LTRs from whom samples from two pairs were available, both were analysed.

**B:** The table shows the number of mixed sample pairs that presented the respective dynamics, increase in gt number, or change in gt frequency, or both (total dynamics). Antiviral medication was considered when given between or at time of analysed time points as a fraction of all pairs in this group.

**C:** For statistical tests, one sample pair per patient (the earliest one tested) was included ( $n = 27$ , Fisher's exact test; \*\* for  $P < 0.01$ ). Total dynamics was significantly higher in D+ patients compared to D- patients ( $P = 0.0061$ ), while the increase in gt number and change in gt frequency did not reach significance ( $P = 0.0899$  and  $P = 0.2087$ ; respectively).  
gt, genotype; D, donor; R, recipient; ns, non-significant

#### 148 *Two patterns of genotype predominance dynamics over time*

149 The predominance change in relative genotype frequency displayed two distinct patterns. First, an  
150 exchange of the pre-existing genotype (thereby an initially minor genotype becomes the major), and  
151 second, the introduction of a new genotype that overtakes the previously predominant genotype  
152 (whereby the initially major genotype becomes undetectable or a minor). While paired BAL samples  
153 ( $n = 10$ ) presented both predominance patterns equally frequent, all plasma sample pairs ( $n = 6$ )  
154 displayed the second pattern, introduction of a new predominant genotype (Supplementary Table 2).  
155 Overall, a change in predominance was detected the earliest 62 days after the first episode, indicating  
156 that intra-host dynamics can be rapid.

157

158 **The pre-transplant donor lung may harbour multiple genotypes**

159 To learn more about the donor lung as a potential HCMV source, we analysed the middle lobe part of  
160 ten lungs of HCMV-seropositive donors for HCMV-DNA positivity and genotype diversity. Of each  
161 middle lobe, one to eight different locations were collected (Supplementary Table 3a). Each individual  
162 tissue piece was stored in buffer before being processed to a single cell suspension (details see  
163 Materials and Methods). In total, 60 lung pieces and the corresponding storage buffer samples were  
164 tested for HCMV positivity. We detected HCMV-DNA in 8/60 cell suspensions and in 15/60 storage  
165 buffer samples. Frequent detection of HCMV-DNA in storage buffer is most likely due to release of  
166 HCMV-DNA from damaged cells and/or blood vessels during collection. In summary, five out of the  
167 ten lung donors were HCMV-DNA positive. Two out of ten donors were HCMV-DNA positive in the  
168 cells only, two donors were positive in the storage buffer only and one donor was positive in both,  
169 cells and storage buffer. In the cellular fractions, we detected HCMV-DNA in up to four out of eight  
170 different locations (Supplementary Table 3a). These findings indicate focal HCMV-DNA distribution  
171 in the analysed lung tissues. All HCMV-DNA positive samples were subjected to short amplicon  
172 genotyping. We detected up to three genotypes in a single donor sample and three out of four donors  
173 displayed mixed genotypes (Supplementary Table 3b). These findings show that multiple HCMV  
174 strains are transmittable with the donor lung, thus may substantially contribute to an increased HCMV  
175 strain diversity post-transplantation.

176 **Long-read PacBio sequencing for haplotype analysis**

177 Thus far, we have assessed HCMV strain diversity and dynamics based on sequencing data of short  
178 polymorphic regions to define the respective HCMV genotypes. To expand our understanding on  
179 within-host HCMV strain diversity we quantitatively determined the individual haplotypes in a subset  
180 of 23 BAL and one EP sample from 20 LTRs by long-read PacBio sequencing. Sample selection was  
181 restricted by the viral load sensitivity limit of the long-read PCR (for details refer to Materials and  
182 Methods). Herein, the term haplotype refers to a single HCMV genome of > 6kb covering multiple  
183 non-adjacent genotype-defining regions.

184 Long amplicons were generated from four regions, F5, F1, F3 and F4 (Figure 1) and subjected to  
185 long-read PacBio sequencing similarly as described previously (Brait et al., 2022). The amplicon  
186 fragments range between 6.2 and 7.9 kb in length and cover all polymorphic genes (dN,  
187 nonsynonymous substitutions per nonsynonymous site  $\geq 0.086$ ) we used for genotyping and 15 more.  
188 These include seven of the most divergent HCMV genes (dN  $\geq 0.034$ ) and two less variable genes  
189 UL55 (gB) and UL75 (gH), extensively sequenced in previous studies due to their known functional  
190 importance (Sijmons et al., 2015). Detailed information on PacBio-determined haplotypes are  
191 presented in Supplementary Table 4a. In Figure 5A the assignments of the identified haplotype  
192 sequences to the most similar reference sequences are displayed. Ten LTRs were single haplotype  
193 infected, nine LTRs were infected with up to two haplotypes, and in one patient (LTR-45) up to three  
194 haplotypes were detected. In total, we identified 116 individual haplotypes in 20 LTRs and for each,  
195 sequences with identities  $>98\%$  were found in the NCBI Nucleotide (nr/nt) database (Supplementary  
196 Table 4b), except for four haplotypes sharing only 93% to 96% identity. Notably, for 38% of the 165  
197 reference sequences corresponding haplotype sequences were found in our cohort illustrating a  
198 substantial inter-host haplotype diversity. Despite a high inter-host variability, we found haplotypes in  
199 different patients sharing sequence identities of up to 99.9% and 99.8% in F3 and F5, respectively  
200 (6A\_hap1, 12B/F\_hap1) and 99.7% in F1 (16B\_hap2, 45B/D\_hap2). Haplotypes of F4 were more  
201 diverse with a maximum of 98.5% sequence identity between haplotypes 11O\_hap1 and 37B\_hap1.

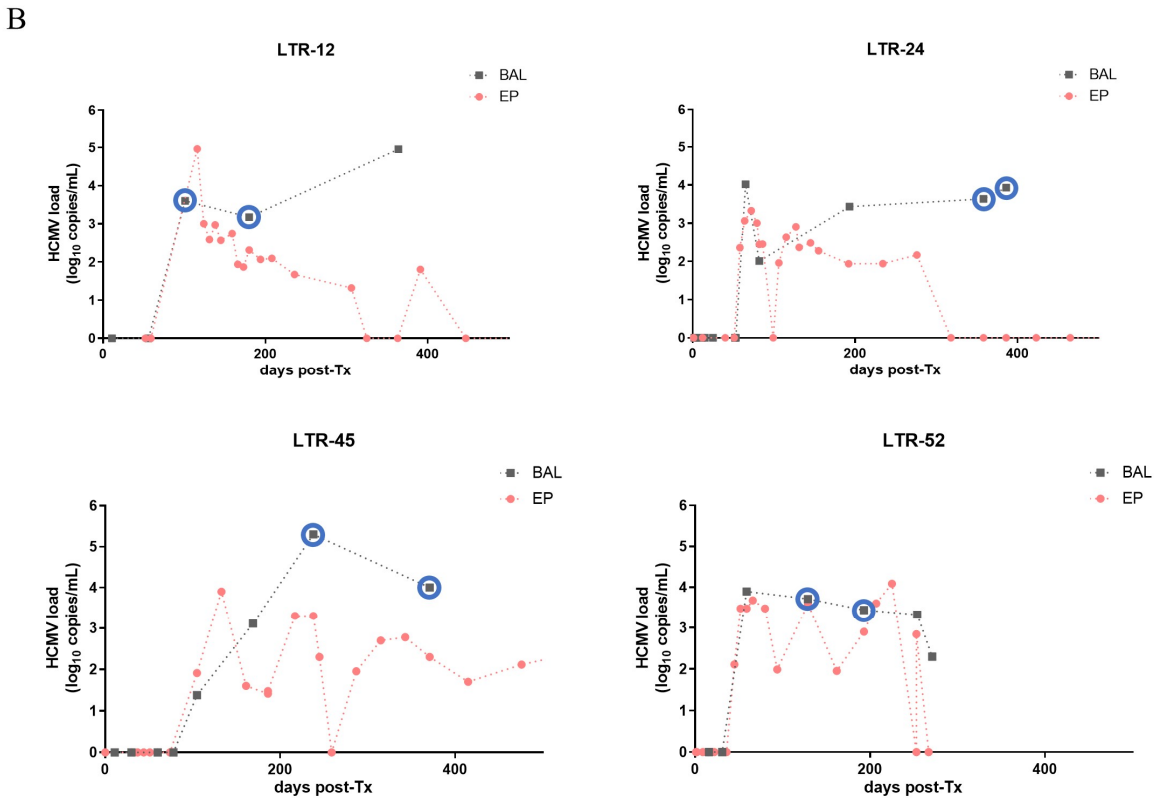
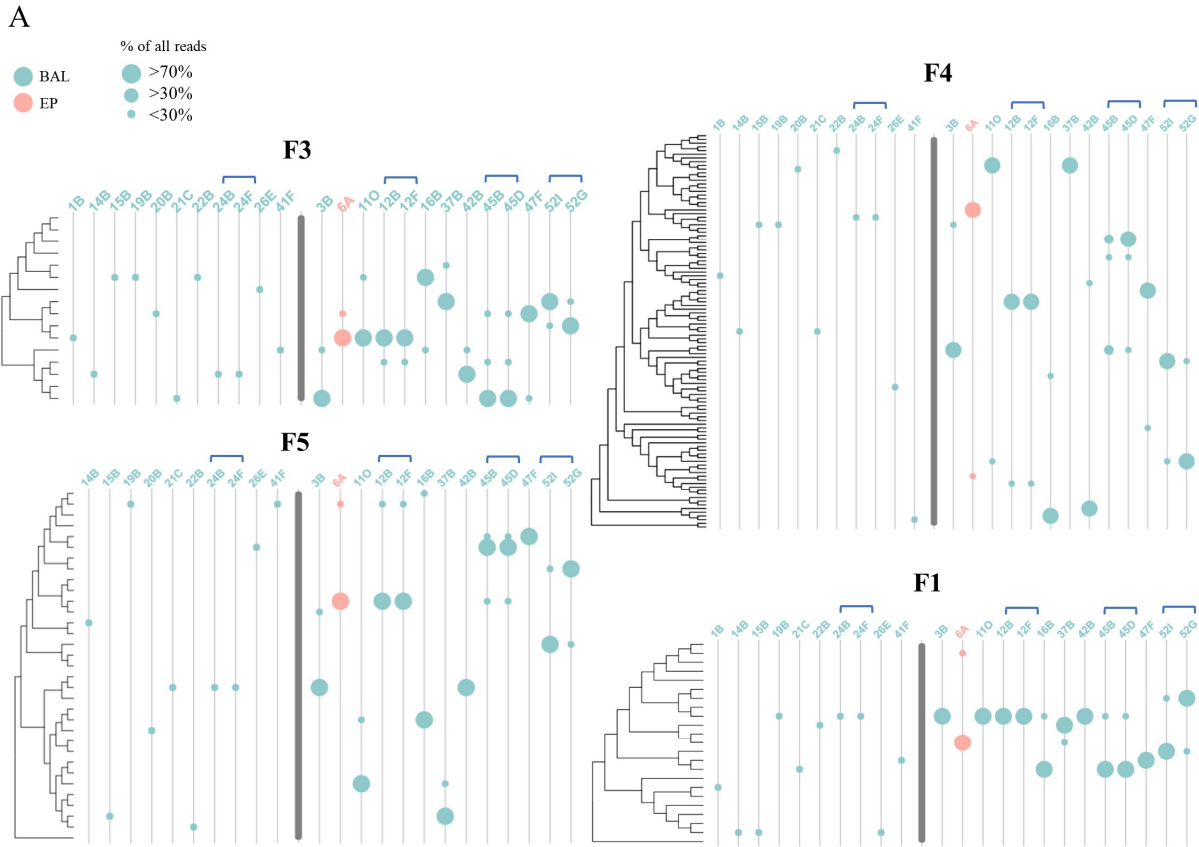


**Figure 5. A: Graphical representation of the 144 detected haplotypes of the four long amplicon regions.** The trees cluster representative haplotypes of the respective regions that differ in >150 nucleotides based on all publicly available HCMV strains (accession numbers are provided in Supplementary Table 7a). Distances are in the units of the number of base differences per sequence. Trees were generated in MEGA X using the UPGMA method and displayed with Evolview. Single and mixed infected samples are separated by a bold grey line. Samples 24B/F, 12B/F, 45B/D and 52I/G are follow-up samples of the same patients and are indicated with blue brackets.

**B: HCMV viral loads of longitudinal samples from BAL and EP from LTRs 12, 24, 45 and 52.** Blue circles indicate samples that have been subjected to PacBio long-read sequencing.

BAL, bronchoalveolar lavage; EP, EDTA-Plasma; LTR, lung transplant recipient; post-Tx, post-transplantation



204 ***Rapid intra-host dynamics, but stable haplotype sequences over time***

205 For four LTRs two follow-up BAL samples each were included (Fig. 5A; indicated with blue brackets)  
206 to assess the haplotype dynamics over time. The course of HCMV-DNAemia for these four patients is  
207 provided in Figure 5B. First, one patient (LTR-24) was single haplotype infected showing the same  
208 haplotypes in both samples (24B, 24F; time between samples ( $\Delta$ ): 28 days). Second, the longitudinal  
209 samples 52I and 52G ( $\Delta$ : 64 days) of LTR-52 illustrate the change in predominance of the two  
210 haplotypes from time points 1 to 2 throughout all four regions. Third, samples 12F and 12B ( $\Delta$ :79  
211 days) of LTR-12 show the same two haplotypes with consistent relative frequencies for both time  
212 points. Fourth, for patient LTR-45 a change in predominance of the major haplotype is only observed  
213 in region F4 ( $\Delta$ :133 days). Alignments of the within-patient haplotype sequences show 100%  
214 sequence identity except for the minor haplotypes of samples 45B and 45D for the region F1  
215 (45B/D\_F1\_hap2) and a suspected fourth haplotype for region F4 (45B\_F4\_hap4). Here, a closer look  
216 reveals that 45B/D\_F1\_hap2 consists of a mixture of two sub-haplotypes with 12 nucleotide  
217 differences (Supplementary Table 4c). Separation of the two sub-haplotype sequences show that both  
218 sub-haplotypes are present in samples 45B and 45D and the respective sequences are 100% identical  
219 in both samples. The sequence of haplotype 45B\_F4\_hap4, in contrast, is different. Visual inspection  
220 of the individual PacBio circular consensus sequence (ccs) reads revealed two different groups of ccs,  
221 both sharing sequence similarity with haplotype sequences 45B\_F4\_hap1 and 45B\_F4\_hap2 (Figure  
222 6-figure supplement 1). The two groups with 12 and 15 ccs reads each display recombined sequences  
223 with breakpoints upstream and downstream of coding sequence (CDS) of UL144, respectively.  
224 PCR-mediated recombination cannot be ruled out, thus, these sequences were excluded from further  
225 analysis. In summary, the longitudinal haplotype data show, as observed for the genotyping data, that  
226 changes in predominance can be fast-paced, while the haplotype sequences remain stable.

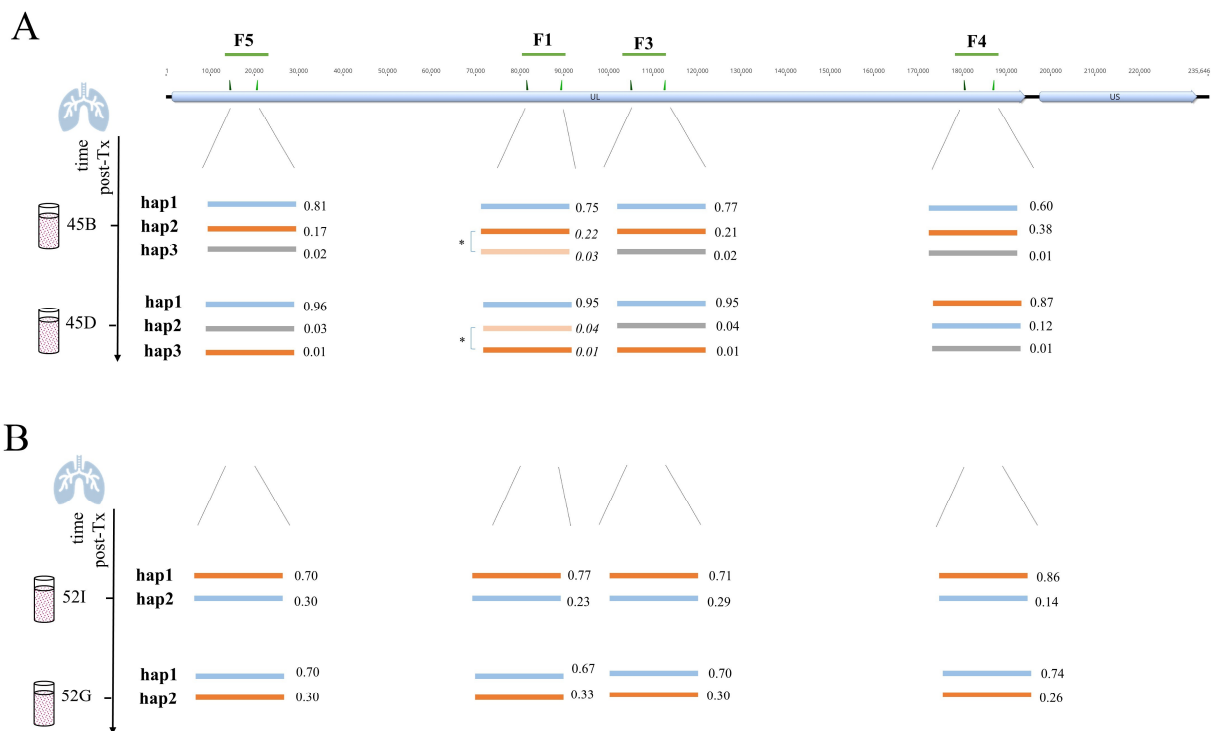
227 ***Genotypes shared between intra-host haplotypes limit overall diversity in mixed samples***

228 To investigate how linkage combinations between non-adjacent polymorphic regions contribute to  
229 intra-host diversity in mixed strain samples, we compared the number of genotypes of eight highly  
230 polymorphic genes ( $dN \geq 0.082$ ) with the number of haplotypes in these regions. In total, 10 mixed  
231 infected LTRs with 75 distinct haplotypes were analysed. Genes used for genotype determination were

232 gN and gO in F3, UL139, UL144 and UL146 in F4 and UL6, UL9 and UL11 in F5 (Figure 1). For  
233 region F3, in all samples the number of genotypes matched the number of haplotypes, possibly  
234 because of the well-described linkages between gN and gO genotypes restricting recombination and  
235 consequently different linkage combinations (Mattick et al., 2004). All haplotypes in our cohort  
236 showed previously described gN/gO linkages. In three LTRs fewer genotypes than haplotypes were  
237 observed in target regions F4 and F5, suggesting different linkage patterns (Supplementary Table 5).  
238 First, we identified two F5 haplotypes in sample 3B, both sharing the UL11-2 genotype with only one  
239 nucleotide difference in the 429 bp long region used for UL11 genotyping. Pairwise alignments of the  
240 two F5 haplotypes clearly show substantial differences across the full 6.4 kb sequence with stretches  
241 of high identity in UL11 CDS (Figure 6–figure supplement 2A). Second, we found two F4 haplotypes  
242 in sample 11O, but only one UL139-2 genotype with 14 nucleotide differences (98% identity) across  
243 the genotyping region (Figure 6–figure supplement 2B). Lastly, in both samples of LTR-45 (45B/45D)  
244 three F4 haplotypes, but two UL139, UL144 and UL146 genotypes and three F5 haplotypes, but two  
245 UL6, UL-9 and UL11 genotypes were found. Again, haplotypes differed in one and up to 11  
246 nucleotides in the respective genotyping regions, but considerable differences up-and downstream  
247 confirmed distinct haplotypes (Figure 6–figure supplement 2C and 2D). Interestingly, while the same  
248 UL139 genotype was shared between hap1 and hap2, the same UL144 and UL146 genotypes were  
249 found between hap2 and hap3, which is indicative of past recombination. Of note, intra-host  
250 haplotypes in our cohort shared up to 40% identical sequence sections, which is ideal for homologous  
251 recombination (Figure 6-figure supplement 3). Taken together, the full haplotype sequence allowed a  
252 clear determination of distinct haplotypes, although same genotype assignments were found.

253 While linkage patterns of non-adjacent genotypes within a haplotype region can unambiguously be  
254 defined by long read sequencing, linkages of non-overlapping haplotypes might be assessed according  
255 to their relative frequencies (Brait et al., 2022). We refer to this as a statistical linkage of haplotypes  
256 (relative frequencies of all haplotypes are provided in Supplementary Table 4a). As illustrated in  
257 Figure 6B for patient LTR-52 it can be assumed that the major (hap1) and minor (hap2) haplotypes,  
258 respectively, are present on the same HCMV genome. Moreover, the statistical linkage remained  
259 stable even after the predominance change from time point 1 to 2. For samples with varying relative

260 frequencies of the distinct haplotypes of each region, direct statistical linking is not reasonable. The  
 261 longitudinal samples 45B/45D shown in Figure 6A, exemplify this problem clearly. First, in both  
 262 samples the relative haplotype frequencies were similar for the regions F5, F1, and F3, but not for F4.  
 263 Second, the major haplotype of F5, F1, and F3 did not change over time, but the major haplotype of  
 264 F4 did. Third, relative frequencies of the haplotypes, hap2 and hap3 were only similar for F5, F1, and  
 265 F3, but not for F4. Thus, the three individual haplotypes of F5, F1, and F3 can be statistically linked,  
 266 but no further linkage with the F4 haplotypes is feasible. These data may indicate that more than three  
 267 unique HCMV strains are present in these samples, probably resulting from recombination in between  
 268 the target regions F3 and F4.



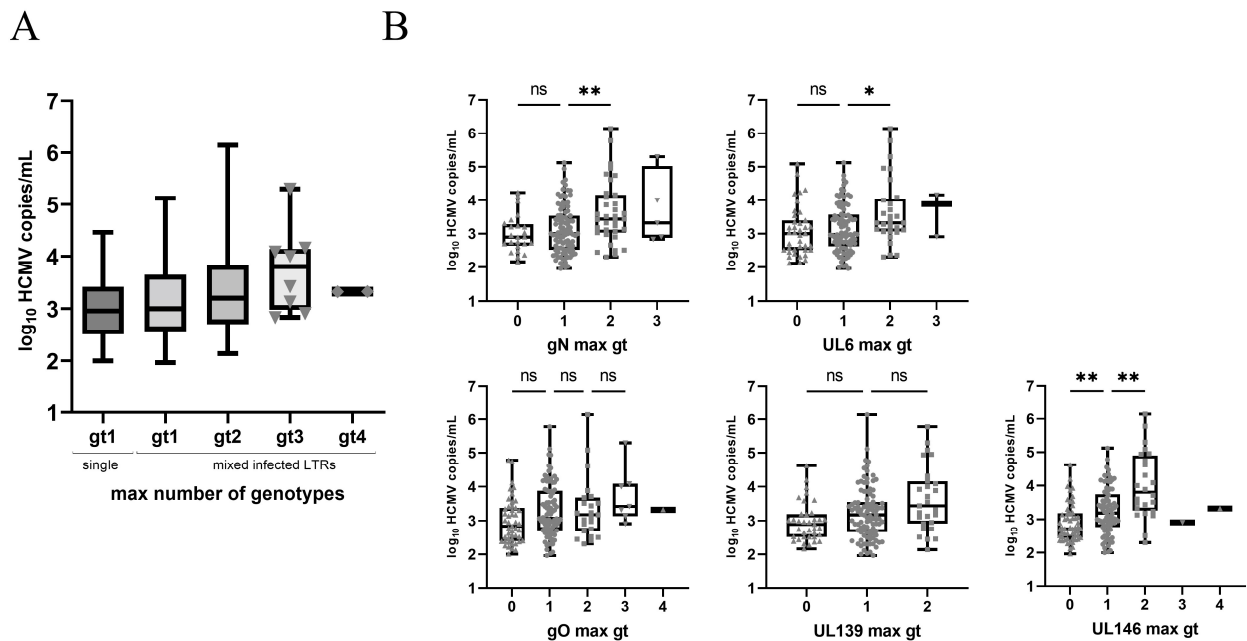
269

**Figure 6. Schematic presentation of haplotypes of longitudinally PacBio sequenced BAL samples of LTR-45 (A) and LTR-52 (B).** The top track shows the overall HCMV genome structure that consists of a unique long (UL) and a unique short (US) region with the long amplicon target regions (F5, F1, F3, F4) depicted as green lines. Haplotypes determined for each of the four long amplicon regions are presented as lines of different colours. The values next to each haplotype are the relative frequencies of the respective haplotype.

**A:** The two sub-haplotypes of LTR-45 of region F1 (marked with an asterisk) were initially detected as a single haplotype (hap2), since they only differed in 12 nucleotides across the whole fragment (further details in Results and Supplementary Table 4c). Here, there are shown as separate haplotypes and the calculated relative frequencies are shown in italic.

**B:** For LTR-52, similar relative frequencies of both haplotypes of each region suggest their statistical linkage. A change in predominance is observed between both time points and support that orange and blue haplotypes are linked, respectively.

post-Tx, post-transplantation; nt, nucleotide



271

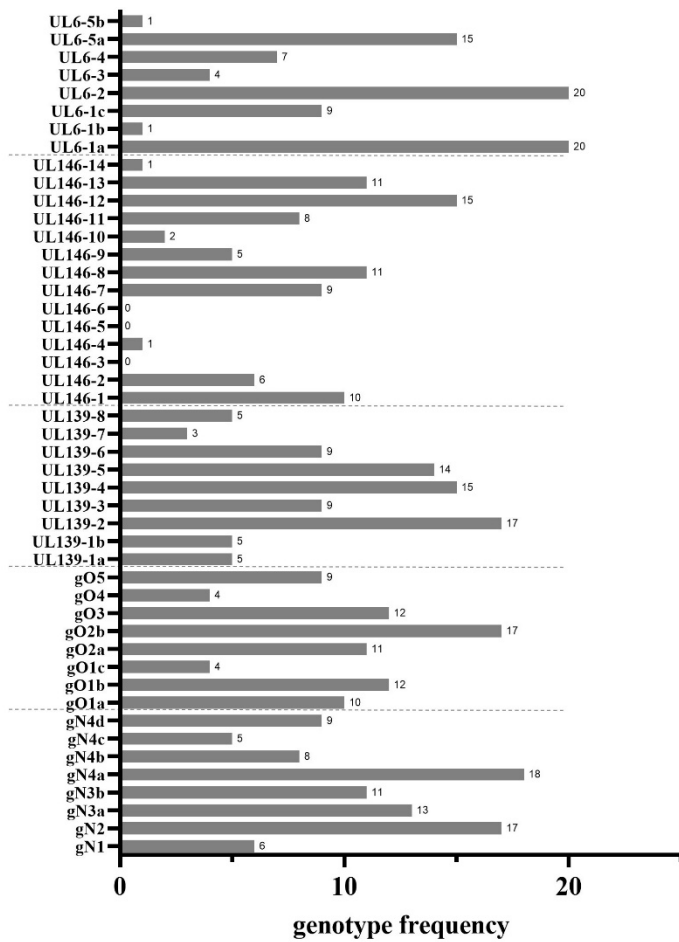
**Figure 2—figure supplement 1. Box and whisker plots of the HCMV viral load (VL) and the maximum number of genotypes (max gt) detected for all five loci or for gN (UL73), gO (UL74), UL139, UL146 and UL6 separately.**

**A:** A trend towards higher VL with increasing gt numbers is observed, but is not significant ( $P = 0.0858$ ,  $n = 161$ ). Symbols show each sample point for groups, where the total  $n$  was  $< 40$ . Single and mixed LTRs are shown separately. In the single group are samples with a single gt at each locus, while samples in group gt1 (mixed infected LTRs) had only one detectable gt in this sample but belong to a mixed infected patient.

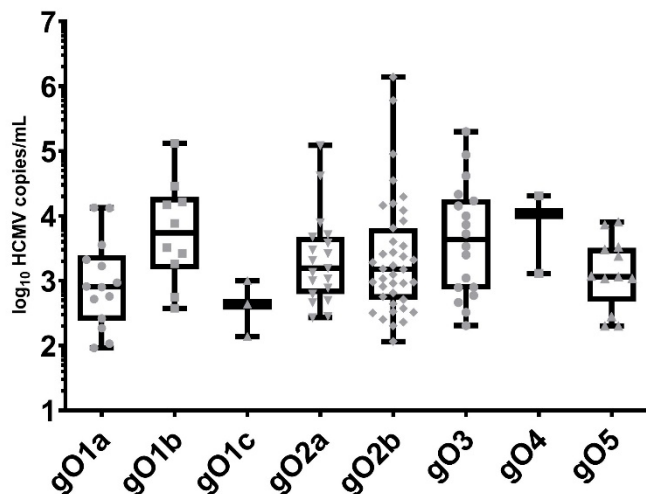
**B:** All sample points are shown as grey symbols. Max gt 0 shows the VL of PCR-negative samples. VL are significantly higher for samples with max gt = 2 compared with gt = 1, for gN ( $P = 0.0093$ ,  $n = 134$ ) and UL6 ( $P = 0.0490$ ,  $n = 122$ ). For UL146 PCR, samples with max gt = 0 compared with max gt = 1 and max gt = 1 compared with max gt = 2 are also significantly different in their VL ( $P = 0.0075$ ,  $n = 137$  and  $P = 0.0031$ ,  $n = 106$ , respectively).

Kruskal-Wallis test with *post hoc* Dunn's multiple comparison test was applied for samples with  $n > 5$  (\* for  $P < 0.05$ ; \*\* for  $P < 0.01$ )

ns, non significant; LTR, lung transplant recipient; gt, genotype



272 **Figure 2—figure supplement 2. Normalised frequencies of all genotypes of five polymorphic loci in 50 lung transplant**  
 273 **recipients (LTRs).** If a certain genotype occurred multiple times in different samples of the same LTR, it was counted once  
 for this analysis (normalised frequency). Both, plasma and bronchoalveolar lavage samples are included. We find all  
 genotypes except for UL146-3, UL146-4 and UL146-6.



274 **Figure 2—figure supplement 3. Major gO genotypes detected in 50 lung transplant recipients.** Only major  
 genotypes (defined as >70% of all reads) are shown and used for analysis, since the major strain is expected to  
 contribute the most to the total viral load. No significant difference between viral loads and genotypes were found in  
 a Kruskal-Wallis test with *post hoc* Dunn's multiple comparisons test for groups with n > 5 ( $P = 0.1189$ , n = 112).

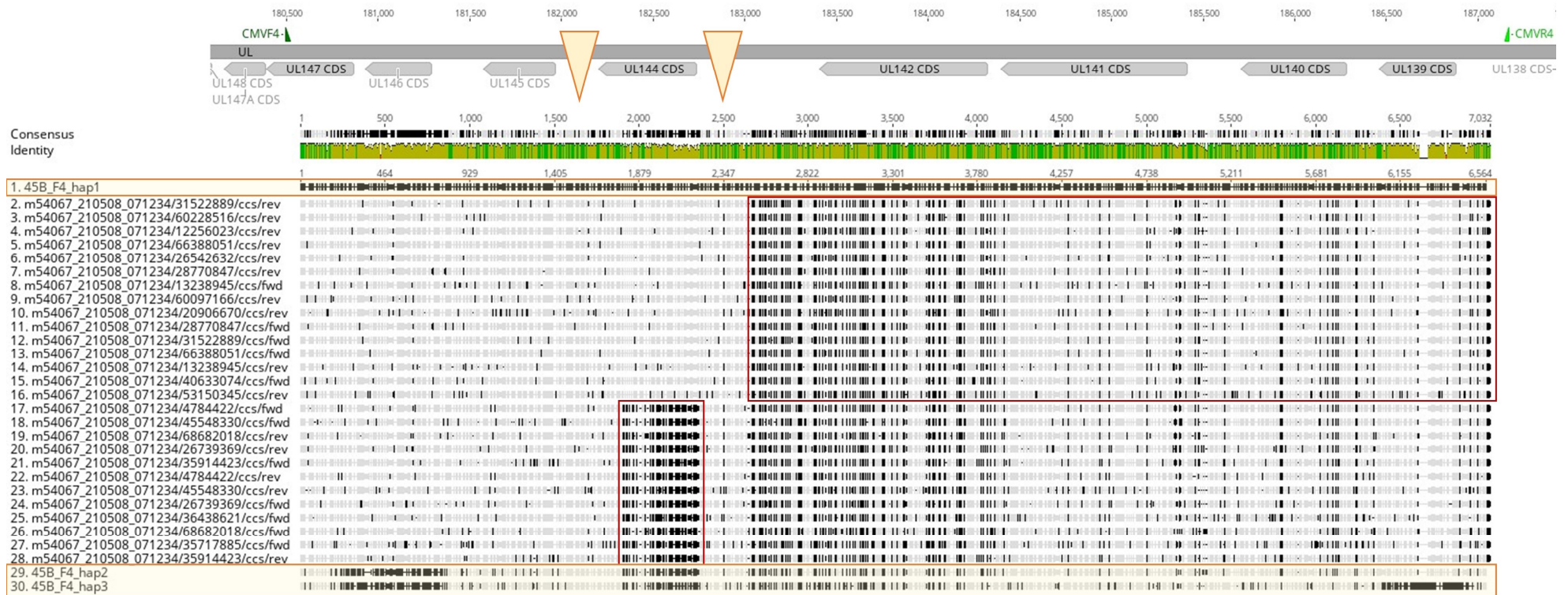


**Figure 6–figure supplement 1. Alignment of the three haplotypes of sample 45B of region F4 (45B\_F4\_hap1, 45B\_F4\_hap2 and 45B\_F4\_hap3) with the PacBio circular consensus reads (ccs) that were initially aligned to the fourth haplotype 45B\_F4\_hap4.**

The upper track displays the coding sequences (CDS) along the 6.6 kb F4 amplicon region, below the mean pairwise identities of the aligned sequences are shown in green (100%), brown (≥30% < 100%) and red (≤30%). Orange triangles indicate potential breakpoint regions for recombination. Then, the alignment of 30 sequences is shown with hap1 set as reference (top sequence marked in orange). The sequences between the orange highlighted haplotypes at the very top (hap1) and bottom (hap2 and hap3) are the 27 ccs reads belonging to hap4 in the first round of mapping. This alignment illustrates that the haplotype sequences that were used to construct the consensus sequence of hap4 actually consists of two groups and indicate two regions of recombination. The upper 15 ccs reads show similarities to hap1 before switching to hap2 around the position of the 2<sup>nd</sup> triangle. The other 12 reads switch at the 1<sup>st</sup> triangle. Red boxes show where the change into the pattern of hap2 occurs.



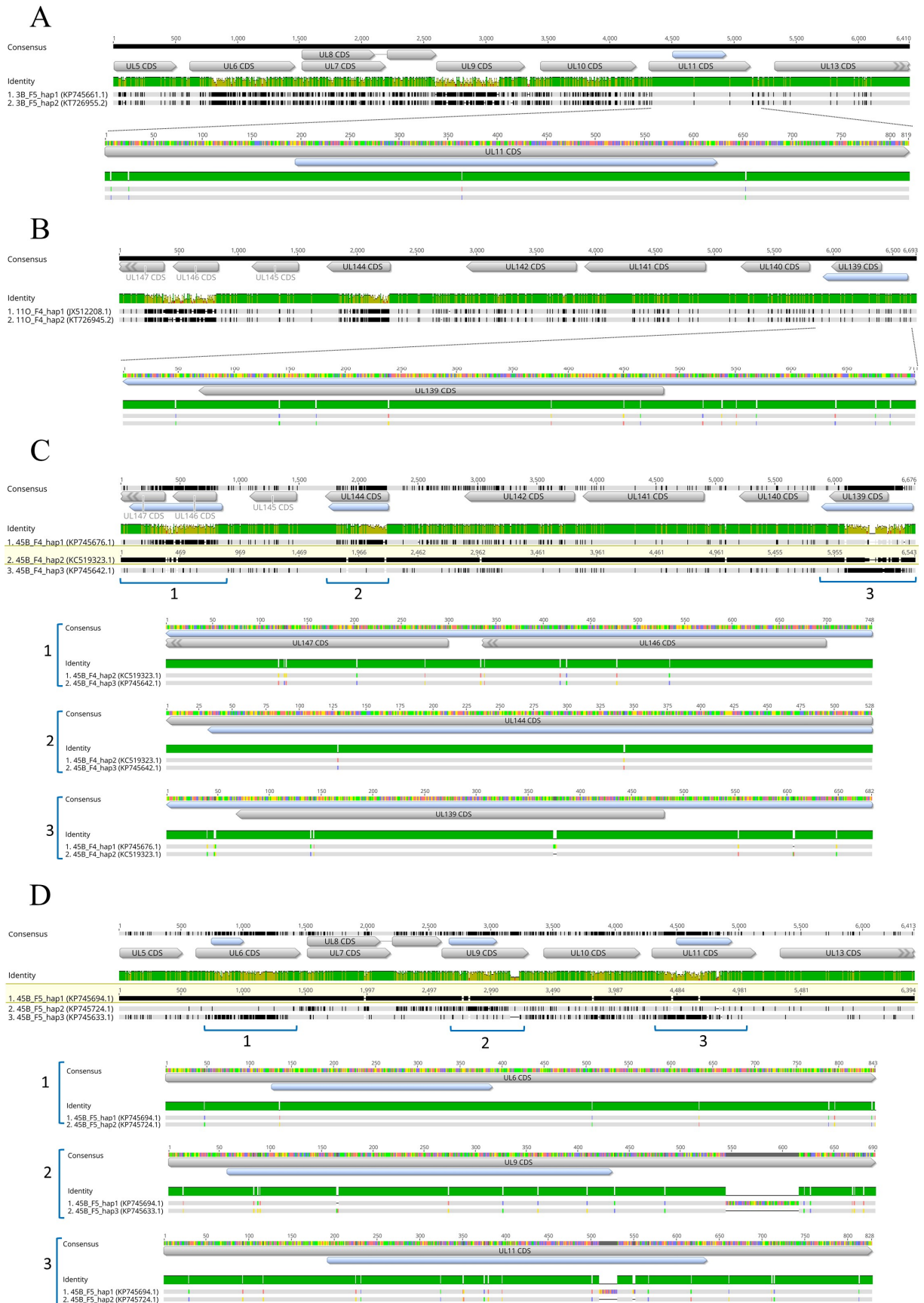


**Figure 6-figure supplement 2. Alignments of intra-host haplotypes of samples 3B (A), 110 (B), 45B F4 (C) and F5 (D) show minor differences in genotype-defining regions.** In the upper track the coding sequences (CDS) are displayed in gray boxes. The regions used for genotype determination are shown in light blue. Below, the mean pairwise identities of the aligned sequences are shown in green (100%), brown ( $\geq 30\%$  - $<100\%$ ) and red ( $\leq 30\%$ ). Next, intra-host haplotypes are aligned and differences shown with black lines, with one haplotype set as reference in C and D (highlighted in yellow). In the zoom-in sections below, the two haplotypes sharing genotypes in the respective region are pairwise aligned and the nucleotide differences are shown in colours corresponding to the respective nucleotide (green, thymine; blue, cytosine; red, adenine; yellow, guanine).

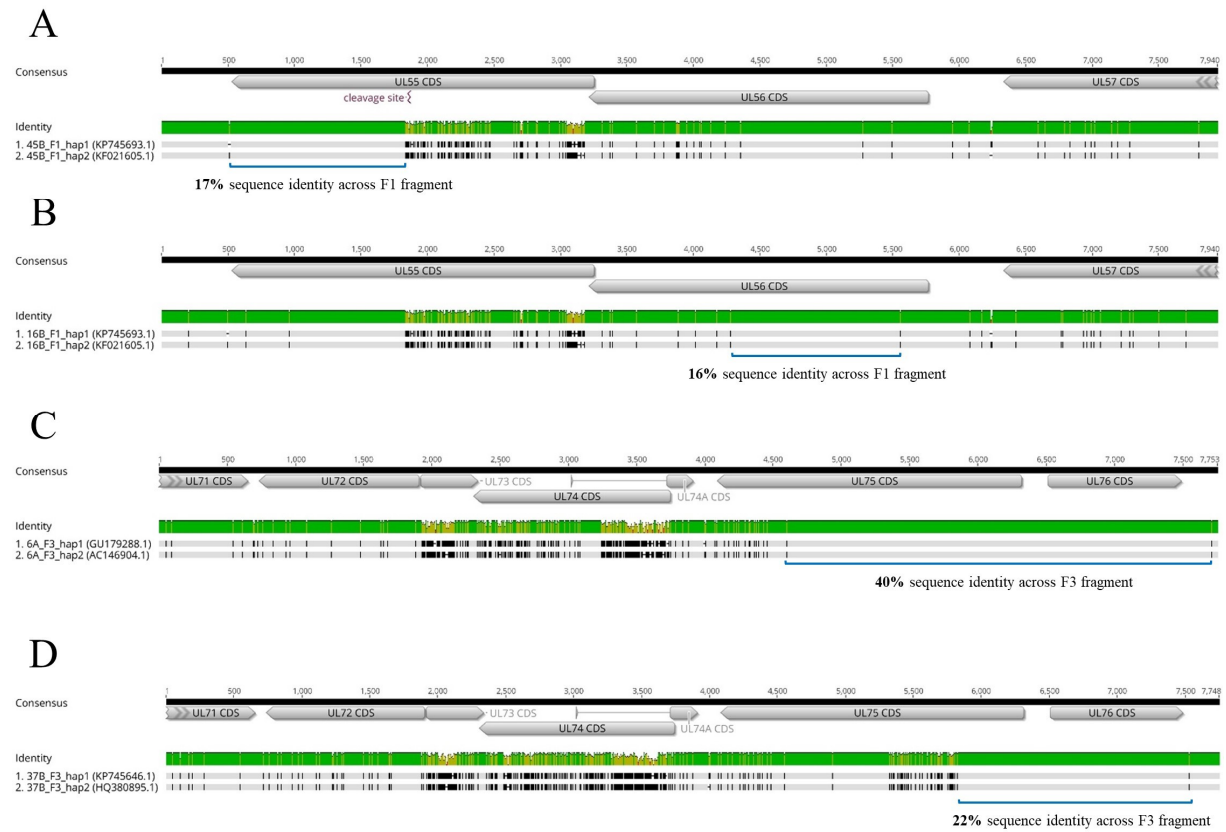


**Figure 6–figure supplement 3. Sequence alignments of intra-host haplotypes of samples 45B, 16B, 6A and 37B show long stretches of sequence identity.** In the upper track the coding sequences (CDS) are displayed in gray boxes. The regions used for genotyping are shown in light blue and the cleavage site in gB is marked. Below, the mean pairwise identities of the aligned sequences are shown in green (100%), brown ( $\geq 30\%$  - $<100\%$ ) and red ( $\leq 30\%$ ). Lastly, intra-host haplotypes are pairwise aligned and differences shown with black lines.



## Discussion

In this study, we have comprehensively assessed the diversity and replication dynamics of mixed HCMV strains in patients with multiviremic HCMV episodes after lung transplantation. We identify the donor lung as a critical source for a complex and dynamic HCMV strain population independent of the recipients' HCMV serostatus and we demonstrate that distinct genotype linkage combinations may not necessarily increase the overall intra-host diversity.

Sensitive and quantitative assessment of HCMV genome diversity directly from clinical material is important to study the composition and dynamics of mixed infections robustly. Due to the low amount of starting HCMV-DNA in clinical specimens, PCR-amplicon enrichment followed by short-read Illumina deep-sequencing was performed. Previous studies using PCR-based approaches confirmed that the detection of mixed strains could depend on the viral load, the genetic loci and clinical specimen type analysed (Görzer et al., 2008)(Sowmya & Madhavan, 2009)(Manuel, Åsberg, et al., 2009). We were able to analyse samples with viral loads starting from  $10^2$  copies/mL and detect minor variants down to 1%, making this approach explicitly more sensitive for detection of mixed infections compared to a whole genome sequencing approach (Suárez, Wilkie, et al., 2019). The five genes (UL6, gN, gO, UL139 and UL146) we chose are among the 12 highest polymorphic ones with a  $dN \geq 0.086$ , are predicted to encode for products of immunomodulation and are known to be necessary for cell entry (Sijmons et al., 2015)(Wang et al., 2021)(Bradley et al., 2008). While the high overall genotyping success rates (67-85%) confirm that these target regions are very well suitable to determine genotypic diversity the data also show that HCMV-DNA isolated from BAL samples is better amplifiable than from plasma samples (Figure 2A). This is most likely due to the high fragmentation of plasma HCMV-DNA as previously suggested (Tong et al., 2017)(Brait et al., 2022). This also explains why amplicons of  $> 6$ kb, which were used for long read sequencing, could hardly be generated from plasma-derived HCMV-DNA, despite similar viral load concentrations as in BAL samples.

In our cohort of 50 lung transplant patients, we found representatives of almost all genotype sequences (41 out of 44), yet with varying prevalences. No specific genotype was associated with significantly

higher or lower viral loads, suggesting that genotypic variations do not affect HCMV replication efficiency (Figure 2–supplement 2). Three UL146 genotypes, gt3, gt5 and gt6, were not present in our study cohort (Figure 2–supplement 3). This is well in accordance with prior studies also reporting a low frequency for these genotypes (Bradley et al., 2008)(Berg et al., 2021). UL146 ORF encodes a viral  $\alpha$  (CXC)-chemokine, that is suggested to recruit neutrophils for viral dissemination (Lüttichau, 2010). A recent study investigated the functional variability of distinct recombinant UL146 proteins showing that UL146 polymorphisms differentially affect chemokine receptor binding affinity, which could influence HCMV dissemination and pathogenesis (Heo et al., 2015). Hence, it might be speculated that the absence of UL146 gt3, gt5, and gt6 in this cohort is due to a lower virulence compared to the other genotypes. In general, cellular CXC chemokines are divided into two groups depending on the presence or absence of an ELR (Glu-Leu-Arg) motif prior to the CXC motif with an angiogenesis promoting and inhibiting function, respectively. Interestingly, all UL146 genotypes that have been detected in our cohort share this ELR motif but not the missing genotypes gt5 and gt6 (Heo et al., 2008). High levels of ELR chemokines have been suggested to be major mediators of lung disease processes such as bronchiolitis obliterans syndrome (BOS), adult respiratory distress syndrome and pulmonary fibrosis (Belperio et al., 2005)(Keane et al., 2002)(Keane et al., 1997). It can be speculated that increased activity of viral ELR chemokine homologues in the lung could change the balance between angiogenic or angiostatic chemokines in favour of aberrant angiogenesis. This might play a role in why HCMV replication is a risk factor for BOS development (Paraskeva et al., 2011), and might be worth to be addressed in future studies.

A main objective of this study was to identify the relationship between pre-transplant D/R HCMV serostatus and strain diversity and dynamics post-transplantation. The finding that D+R+ patients harbour a higher number of genotypes compared to the other two D/R groups (Figure 3B) indicates that both, donor- and recipient-derived strains contribute to the observed diversity. Although several previous studies found that reinfection with donor-derived strains are more common than reactivation of recipient virus (Grundy et al., 1988)(Chou, 1986)(Sunwen & Norman, 1988), others have argued that infections post-transplantation are approximately equally donor- and recipient-derived (Manuel, Pang, et al., 2009). Reports on the detection of HCMV in tissues of non-immunocompromised

individuals (Schonian et al., 1993)(Kytö et al., 2005)(Kraat et al., 1992)(Hendrix et al., 1997)(Meyer-König et al., 1998) further underline the potential of HCMV transmission with the allograft, yet the extent of transmission remained controversial. In the present study, we could demonstrate HCMV-DNA positivity in 5/10 pre-transplant lungs of HCMV-seropositive donors, with up to three HCMV genotypes present in small HCMV-DNA positive tissue sections of a single donor lung. Assuming that the detected HCMV-DNA reflects replicating rather than latent HCMV-DNA, these findings indicate focal points of HCMV reactivation of either a single or multiple HCMV strains. Of note, in the HCMV-positive cases reactivation must have started already before surgical organ removal, which is likely given that all donors were in the intensive care unit and under ventilation for >24 hours. Interestingly, the focal distribution of HCMV-DNA in the human lung resembles the murine CMV infection model in which the authors also observed a ‘patchwork pattern’ of focal reactivation and recurrence (Kurz et al., 1999)(Kurz & Reddehase, 1999). Taken together, our data strongly support the findings that HCMV transmission by the allograft of an HCMV-seropositive donor is very likely, yet either the extent thereof or whether it occurs or not may vary among donors. In our present study 2/15 D+R+ patients analysed longitudinally were solely infected with a single HCMV strain despite an overall higher diversity in this patient group. Nevertheless, our findings point towards the donor’s lung as an important contributor to HCMV strain transmission in both HCMV seropositive and seronegative recipients. Strategies to target this reservoir in pre-transplant lungs of HCMV seropositive donors are promising. Recently, the ‘shock and kill’ approach in which latent cells are targeted and cleared has been applied to donor lungs. Treatment with the immunotoxin F49A-FTP during ex-vivo lung perfusion has been shown to reduce reactivation to 76% compared to 15% in non-treated, but perfused controls (Ribeiro et al., 2022). We could further show that D+ patients display higher replication dynamics of their mixed HCMV strain populations post-transplantation compared to D- patients, also arguing for the donor-derived strains as the likely cause. It can be speculated that sequential reactivation and dissemination of donor-derived strains post-transplantation can ultimately increase the host’s latency reservoir and gradual reseeded of the lung as well as dissemination into other tissues can contribute to the distribution of HCMV strains (Collins-McMillen et al., 2018). Over time, these processes might result in locally and temporally different replication

levels of the distinct strains. This will either be observed as an increase in the genotype numbers and/or as a change in predominance. The latter dynamics pattern occurs more frequently in D+R+ patients which may be explained by its generally richer pool of strains. A previous study demonstrating the sequential occurrence of different predominant strains in D+R- patients receiving organs from the same donor support our view of sequential and/or stochastic reactivation of donor strains from the graft (Hasing et al., 2021), as has also been proposed by the murine CMV model (Reddehase et al., 1994). Additionally, it is presumable that initial replication of the major strain triggers a strain-specific immune response which might be well controlled thereafter while the initially less prevalent strain becomes predominant in further episodes due to limited cross-protection (Klein et al., 1999)(Wang et al., 2021). Antiviral medication, in contrast, does not substantially interfere with the replication dynamics since no difference in administration of antivirals was observed between patients with and without dynamics or between the different serostatus groups.

In-depth short amplicon sequencing over polymorphic regions is a highly sensitive strategy to decipher mixed genotype infections but may underestimate the true strain diversity due to the small genomic regions analysed and to the lack of information on linkage patterns. To overcome these limitations, we additionally performed long amplicon haplotype sequencing on a subset of 24 samples of 20 patients of whom 10 patients were mixed infected. The four haplotype target regions (F1, F3, F4, F5) cover about 10-fold larger genomic regions than our short amplicon approach. The advantage of long reads to resolve distinct haplotypes in mixed populations became particularly obvious in patients in whom we found haplotypes with partially shared genotypes (Figure 6 – figure supplement 2). Hence, the lack of information on the arrangement of genotypes on individual genomes by short amplicon genotyping approaches, might help to understand why correlating specific genetic variants to clinical observations may lead to inconsistent results (Wang et al., 2021). In one patient, same genotype assignments were shared between hap1 and hap2 in one locus (UL139) and hap2 and hap3 in other loci (UL144, UL146), suggesting that hap2 had arisen by intra-host recombination between hap1 and hap3. The low number of single nucleotide polymorphisms between the same genotypes, which could have been accumulated over time in the patient, would have supported this conclusion. However, the substantial differences across the full length haplotype sequences makes a recent intra-patient generation of a recombinant

haplotype unlikely since within-host haplotype sequences are highly stable on short timescales as shown in our study and by others (Götting et al., 2021)(Dhingra et al., 2021)(Hage et al., 2017)(Cudini et al., 2019). Additionally, almost identical sequences of the respective haplotypes can be found in the database, further pointing towards transmission from another host. Also, identical haplotypes were observed across patients of our cohort and in one patient (LTR-41) we identified a previously described non-recombinant strain, supporting the view that HCMV diversification has occurred early in human history (Suárez, Wilkie, et al., 2019)(Mattick et al., 2004)(Bradley et al., 2008). Both approaches used in our study, short- and long-read sequencing, suggest an upper limit to intra-host HCMV genetic diversity with a maximum of four genotypes and three haplotypes, respectively, in our cohort of lung transplant patients. Although long read sequencing of longitudinal samples is suitable for directly proving within-patient recombination no direct evidence was seen in the analysed genomic regions. Hence, from our data, it appears that the overall within-host HCMV diversity predominantly results from a mixture of genomically distinct strains rather than from newly emerging variants which confirms previous studies (Cudini et al., 2019)(Suárez, Wilkie, et al., 2019)(Suárez et al., 2020).

In conclusion, by HCMV genotype and haplotype determination of clinical samples, we demonstrate the extent to which the donor lung can contribute to HCMV strain diversity and dynamics after transplantation. We suggest that rapid intra-host dynamics of a limited number of HCMV strains might allow quick adaptation to changing environments and less so by enhancing diversity through recombination. Understanding the forces affecting HCMV population diversity and dynamics is an essential step for treatment and vaccine development.

## Materials and Methods

### Study design and sample collection

For this retrospective study, we analysed routine HCMV-DNAemia monitoring data for EP and BAL specimens of LTRs post-transplantation. Between 2016 and end the of 2018, 286 patients received a lung transplant at the Medical University of Vienna. As a standard regimen, all LTRs receive immunosuppressive treatment and antiviral prophylaxis for at least three months post-transplantation. To investigate strain dynamics, we selected for LTRs with 1) at least two active HCMV infection episodes ( $>10^2$  copies/mL) in either EP or BAL and 2) with at least one sample with  $>10^3$  copies/mL (to maximise the chance for long range amplicon PCR). We defined positive HCMV-DNAemia sample points as distinct episodes if between two sample points 1) the viral load declined below  $10^2$  copies/mL or 2) if there was a time interval of three months. All EP and BAL specimens were stored at  $-20^\circ\text{C}$ . Of the total 339 specimens from 53 LTRs that were initially selected, 81 specimens were not available. DNA extraction of 67 was unsuccessful, and PCR amplification of 28 samples resulted in no amplicons. Consequently, three LTRs were excluded. Two to 15 samples were collected from each LTR and sampling time points ranged between four and 1476 days post-transplantation. Clinical information about the patients of the final cohort was retrieved from medical records.

### DNA extraction and viral load quantification

DNA was isolated from 250  $\mu\text{L}$  of BAL or EP samples using the QIAamp Viral RNA Mini kit (Qiagen) as described in the manufacturer's protocol and eluted in 35  $\mu\text{L}$  elution buffer. HCMV DNA was quantified by in-house HCMV-specific qPCR as previously described (Kalser et al., 2017) and stored at  $4^\circ\text{C}$  or  $-20^\circ\text{C}$  for further steps.

### Short and long-range amplicon PCR

Short-range amplicon PCRs for the five polymorphic regions gN, gO, UL6, UL139 and UL146 of HCMV-DNA positive samples were performed as described previously (Brait et al., 2022), but with minor modifications. To save limited DNA material, UL6 and the first step of the nested UL146 PCR was multiplexed. Also, gO PCRs, consisting of three primers, were multiplexed. For samples with low viral loads ( $<10^3$  copies/mL) and sufficient material availability, the usual DNA template amount of 5

$\mu\text{L}$  was doubled. The viral load sensitivity of our long-range PCR was tested for BAL and EP samples (data not shown). Based on that, BAL samples with  $>5 \times 10^3$  copies/mL and EP samples with  $> 5 \times 10^4$  copies/mL were initially amplified with long range PCR. In addition to previously described amplicons F3 and F4 (Brait et al., 2022), F1 and F5 amplicons were designed and tested to cover more polymorphic regions with long reads. F1, F3 and F4 PCR primers were multiplexed. PCR of samples with lower viral loads and EP samples, in general, were performed with the doubled template amount of 20  $\mu\text{L}$ , if available. Samples with unsuccessful long-range PCR were genotyped using short range PCR. All primers are depicted in Figure 1, and Supplementary Table 6 lists detailed descriptions of PCR primers. PCR product lengths were confirmed on analytical agarose gels and concentrations quantified by Qubit prior to Illumina or PacBio library preparation.

### **Illumina and PacBio sequencing**

Library preparation and sequencing for Illumina sequencing were performed as described previously with a few adaptations (Brait et al., 2022). Briefly, amplicons were pooled equimolarly and 2 ng input DNA was used to generate a 4 nM library using the Nextera XT library preparation and index kit, followed by paired-end sequencing (150 cycles, v2 and v2 Micro kits) on an Illumina MiSeq with automatic adapter trimming. Fastq raw reads that passed filters were imported into CLC Genomics Workbench 21.0 (Qiagen) for further analysis.

According to manufacturer's protocol, pooled long range amplicons were purified using the Qiaquick Spin Kit and eluted in 50  $\mu\text{L}$  elution buffer. After quantification and purity determination with NanoDrop 1000 tool (Peqlab) and Qubit 2.0 fluorometer (Thermo Fisher), samples were submitted to the Next Generation Sequencing Facility at Vienna BioCenter Core Facilities for SMRT bell Amplicon library preparation. Sequencing was performed on a PacBio-Sequel system for 20 hours. Twenty-four samples were multiplex sequenced on two lanes.

### **Bioinformatical workflows for PacBio and Illumina reads**

#### ***PacBio CCS generation***

CCS reads were generated from PacBio raw reads using the *ccs* tool (<https://github.com/PacificBiosciences/ccs>) with a minimum predicted read quality of 0.99 (>99%

accuracy) and a minimum of three full passes per strand. To avoid CCS of potential PCR-mediated heteroduplexes of different strains, the *--by-strand* option was used whereby CCS for forward and reverse strands are generated and analysed separately. Next, CCS were demultiplexed using *lima* (<https://github.com/pacificbiosciences/barcoding/>) and resulting bam files imported into CLC Genomics Workbench 21.0.3 (Qiagen) for further analysis.

### ***HCMV haplotype determination***

For each of the four long-range amplicon regions, we compiled reference databases to be used for read mapping. First, we extracted the corresponding amplicon region from 236 publicly available HCMV whole-genome sequences and aligned them using MUSCLE 3.8.31. Pairwise distances were calculated in MEGA X 10.2.4, and only sequences with >150 nucleotide differences in the respective region were filtered for the final reference databases. These resulted in 33, 23, 16 and 93 reference sequences for F5, F1, F3 and F4, respectively (Supplementary Table 7a). Trees were generated in MEGA X 10.2.4 using the UPGMA method and displayed with Evolview v3 (Subramanian et al., 2019) (Figure 5a).

Firstly, human reads were excluded, and reads were length trimmed according to the amplicon length (F1 7.5-7.8 kb; F4 6.45-6.75 kb; F1 7.8-8.1 kb, F5 6.2-6.5 kb). Using the Long Read Support plugin for CLC Genomics (Qiagen), reads were mapped against the filtered reference sequences with default settings and extractions of the consensus haplotype sequences were generated (low coverage threshold: 3, ambiguity code N insertion with the noise threshold set to 0.3 and the minimum nucleotide count to 3). As a control step, all initial, length trimmed reads were re-mapped to the new consensus haplotype(s), and the new consensus sequence was extracted. All final haplotypes of each sample were aligned and checked for their uniqueness. Potential chimeras were inspected visually by checking if final haplotypes could be reconstructed by combining segments of two more abundant haplotypes. Lastly, all unmapped reads of the first mapping of each amplicon were again mapped to all final haplotypes to confirm that all unmapped reads for a certain amplicon belong to any of the other three amplicons.



### ***HCMV genotype determination***

Q30 quality trimmed Illumina fastq reads were filtered for reads >80 bp in length and human genomic reads were excluded. Default mapping parameters were used for match/mismatch scores, insertion/deletion costs, and a length fraction of 0.3 and a similarity fraction of 0.95. Only mappings with >10 reads and a consensus length of at least 75% of the reference sequence were chosen to extract consensus sequences. A noise threshold of 0.3 and a minimum nucleotide count of 3 was applied to insert ambiguity codes (N). All resulting genotype consensus sequences were aligned, screened visually and unique sequences counted as genotypes. PacBio-derived haplotypes were genotyped using blastn (match/mismatch= 2/-3, gap costs = existence 5, extension 2) and a self-assembled BLAST database (Supplementary Table 7b).

For genotyping, five highly polymorphic regions of UL6 (127-388), gO (691-987), gN (1-379), UL139 (187077- 186395, CDS: 1-414) and UL146 (181341- 180571, CDS: 1-360) were used based on sequences provided previously (Suárez, Musonda, et al., 2019). In total, 47 reference sequences were used. For long amplicon reads, genotyping with 34 additional references was performed for regions gH (1-177), UL144 (1-500), UL9 (57-430), UL10 (0-762), UL11 (194-623) and gB (1138-1619). All listed nucleotide positions are in reference to strain Merlin (GenBank: AY446894.2). Reference sequences for genotyping are provided in Supplementary Table 7b.

### **Donor lung tissue processing**

Lung tissues were removed for pre-transplantation size adjustment and would have been discarded otherwise. Middle lobe sections of 1-2 cm<sup>3</sup> of ten HCMV-seropositive donors were collected in phosphate-buffered saline (PBS) and stored at 4°C for processing on the same day (solution termed supernatant, short SN). Bigger sections were divided, and a part submerged in RNeasy<sup>TM</sup> solution (Invitrogen) for storage at -20°C. Next, sections were minced with sterile single-use scalpels, weighted in a 50 mL falcon tube, and digested with Hanks' balanced salt solution supplemented with 0.15% Collagenase D (Roche) for 60 min at 37°C on an orbital shaker at 300 rpm. The tissue solution was diluted with PBS, vortexed vigorously and strained through a 70 µm cell strainer to obtain a single cell suspension. After centrifugation (500 rpm, 10 min, 4°C), red blood cells were lysed with RBC solution

(Invitrogen™ eBioscience™) and the remaining cells were counted using an automated cell counter (Nexcelom). Dead cells were excluded using trypan blue. Both, 1 mL of SN and the single cell suspension (at most  $10^6$  cells) were separately transferred into 2 mL of lysis buffer and eluted in 50  $\mu$ L elution buffer using the bead based NucliSens EasyMagextractor (BioMérieux). HCMV-specific qPCR positive samples were genotyped using short-range amplicon PCRs and the NGS workflow described earlier.

### **Statistical Analysis**

Statistical calculations were performed in GraphPad Prism version 9.0.0.  $P < 0.05$  was considered statistically significant in all tests.

### **Data availability**

Raw sequence data have been deposited in NCBI Sequence Read Archive under BioProject ID PRJNA803978. Haplotype sequences generated in this study and with identities  $< 98\%$  to publicly available sequences were submitted to GenBank with the accession no. OM835733-OM835736 (Supplementary Table 4b).

## **Acknowledgments**

We acknowledge the support and technical assistance of Barbara Jilka, Andreas Rohorzka, Sylvia Malik, Michaela Binder, Barbara Dalmatiner and Gabriele Sigmund. Lastly, we want to thank Sylvia Knapp for her valuable advice.

## **Additional information**

### **Funding**

This work was funded by a grant from the Austrian Science Fund (FWF) to Irene Goerzer (project number: P31503-B26).

### **Declarations**

This study was approved by the Ethics Committee of the Medical University of Vienna under EK-number 1321/2017. All data were pseudonymised before analyses.

## Author contributions

### Author ORCIDs

Büsra Külekçi <https://orcid.org/0000-0002-4074-6021>

Irene Görzer <https://orcid.org/0000-0003-1936-0404>

Nadja Brait <https://orcid.org/0000-0002-9289-3453>

## Additional files

### Supplementary files

Supplementary Tables 1-7b, Supplementary\_Tables\_28022022.xlsx

Transparent reporting form, transparent\_reporting\_28022022.pdf

## Competing Interests

No competing interests declared.

## References

- Almaghrabi, R. S., Omrani, A. S., & Memish, Z. A. (2017). Cytomegalovirus infection in lung transplant recipients. In *Expert Review of Respiratory Medicine* (Vol. 11, Issue 5, pp. 377–383). Taylor and Francis Ltd. <https://doi.org/10.1080/17476348.2017.1317596>
- Belperio, J. A., Keane, M. P., Burdick, M. D., Gomperts, B., Xue, Y. Y., Hong, K., Mestas, J., Ardehali, A., Mehrad, B., Saggari, R., Lynch, J. P., III, Ross, D. J., & Strieter, R. M. (2005). Role of CXCR2/CXCR2 ligands in vascular remodeling during bronchiolitis obliterans syndrome. *Journal of Clinical Investigation*, *115*(5), 1150. <https://doi.org/10.1172/JCI24233>
- Berg, C., Rosenkilde, M. M., Benfield, T., Nielsen, L., Sundelin, T., & Lüttichau, H. R. (2021). The frequency of cytomegalovirus non-ELR UL146 genotypes in neonates with congenital CMV disease is comparable to strains in the background population. *BMC Infectious Diseases*, *21*(1), 1–12. <https://doi.org/10.1186/S12879-021-06076-W/FIGURES/4>
- Bradley, A. J., Kovács, I. J., Gatherer, D., Dargan, D. J., Alkharsah, K. R., Chan, P. K. S., Carman, W. F., Dedicoat, M., Emery, V. C., Geddes, C. C., Gerna, G., Ben-Ismaeil, B., Kaye, S., McGregor, A., Moss, P. A., Puzsai, R., Rawlinson, W. D., Scott, G. M., Wilkinson, G. W. G., ... Davison, A. J. (2008). Genotypic analysis of two hypervariable human cytomegalovirus genes. *Journal of Medical Virology*, *80*(9), 1615. <https://doi.org/10.1002/JMV.21241>
- Brait, N., Külekçi, B., & Goerzer, I. (2022). Long range PCR-based deep sequencing for haplotype determination in mixed HCMV infections. *BMC Genomics*, *23*(1), 31. <https://doi.org/10.1186/s12864-021-08272-z>
- Chou, S. (1986). Acquisition of donor strains of cytomegalovirus by renal-transplant recipients. *The New England Journal of Medicine*, *314*(22), 1418–1423.

<https://doi.org/10.1056/NEJM198605293142205>

- Coaquette, A., Bourgeois, A., Dirand, C., Varin, A., Chen, W., & Herbein, G. (2004). Mixed cytomegalovirus glycoprotein B genotypes in immunocompromised patients. *Clinical Infectious Diseases*, 39(2), 155–161. <https://doi.org/10.1086/421496>
- Collins-McMillen, D., Buehler, J., Peppenelli, M., & Goodrum, F. (2018). Molecular Determinants and the Regulation of Human Cytomegalovirus Latency and Reactivation. *Viruses*, 10(8), 444. <https://doi.org/10.3390/v10080444>
- Cudini, J., Roy, S., Houldcroft, C. J., Bryant, J. M., Depledge, D. P., Tutill, H., Veys, P., Williams, R., Worth, A. J. J., Tamuri, A. U., Goldstein, R. A., & Breuer, J. (2019). Human cytomegalovirus haplotype reconstruction reveals high diversity due to superinfection and evidence of within-host recombination. *Proceedings of the National Academy of Sciences of the United States of America*, 116(12), 5693–5698. <https://doi.org/10.1073/pnas.1818130116>
- Dhingra, A., Götting, J., Varanasi, P. R., Steinbrueck, L., Camiolo, S., Zischke, J., Heim, A., Schulz, T. F., Weissinger, E. M., Kay-Fedorov, P. C., Davison, A. J., Suárez, N. M., & Ganzenmueller, T. (2021). Human cytomegalovirus multiple-strain infections and viral population diversity in haematopoietic stem cell transplant recipients analysed by high-throughput sequencing. *Medical Microbiology and Immunology*, 210(5–6), 291–304. <https://doi.org/10.1007/s00430-021-00722-5>
- Fulkerson, H. L., Nogalski, M. T., Collins-McMillen, D., & Yurochko, A. D. (2021). Overview of Human Cytomegalovirus Pathogenesis. In *Methods in Molecular Biology* (Vol. 2244, pp. 1–18). [https://doi.org/10.1007/978-1-0716-1111-1\\_1](https://doi.org/10.1007/978-1-0716-1111-1_1)
- Görzer, I., Guelly, C., Trajanoski, S., & Puchhammer-Stöckl, E. (2010). Deep Sequencing Reveals Highly Complex Dynamics of Human Cytomegalovirus Genotypes in Transplant Patients over Time. *Journal of Virology*, 84(14), 7195–7203. <https://doi.org/10.1128/jvi.00475-10>
- Görzer, I., Kerschner, H., Jaksch, P., Bauer, C., Seebacher, G., Klepetko, W., & Puchhammer-Stöckl, E. (2008). Virus load dynamics of individual CMV-genotypes in lung transplant recipients with mixed-genotype infections. *Journal of Medical Virology*, 80(8), 1405–1414. <https://doi.org/10.1002/jmv.21225>
- Götting, J., Lazar, K., Suárez, N. M., Steinbrück, L., Rabe, T., Goelz, R., Schulz, T. F., Davison, A. J., Hamprecht, K., & Ganzenmueller, T. (2021). Human Cytomegalovirus Genome Diversity in Longitudinally Collected Breast Milk Samples. *Frontiers in Cellular and Infection Microbiology*, 11. <https://doi.org/10.3389/fcimb.2021.664247>
- Grundy, J. E., Super, M., Sweny, P., Moorhead, J., Lui, S. F., Berry, N. J., Fernando, O. N., & Griffiths, P. D. (1988). Symptomatic cytomegalovirus infection in seropositive kidney recipients: reinfection with donor virus rather than reactivation of recipient virus. *Lancet*, 2(8603), 132–135. [https://doi.org/10.1016/S0140-6736\(88\)90685-X](https://doi.org/10.1016/S0140-6736(88)90685-X)
- Hage, E., Wilkie, G. S., Linnenweber-Held, S., Dhingra, A., Suárez, N. M., Schmidt, J. J., Kay-Fedorov, P. C., Mischak-Weissinger, E., Heim, A., Schwarz, A., Schulz, T. F., Davison, A. J., & Ganzenmueller, T. (2017). Characterization of human cytomegalovirus genome diversity in immunocompromised hosts by whole-genome sequencing directly from clinical specimens. *Journal of Infectious Diseases*, 215(11), 1673–1683. <https://doi.org/10.1093/infdis/jix157>
- Hasing, M. E., Pang, X. L., Mabilangan, C., & Preiksaitis, J. K. (2021). Donor Cytomegalovirus Transmission Patterns in Solid Organ Transplant Recipients with Primary Infection. *Journal of Infectious Diseases*, 223(5), 827–837. <https://doi.org/10.1093/infdis/jiaa450>
- Hendrix, R. M. G., Wagenaar, M., Slobbe, R. L., & Bruggeman, C. A. (1997). Widespread presence of cytomegalovirus DNA in tissues of healthy trauma victims. *Journal of Clinical Pathology*, 50(1), 59–63. <https://doi.org/10.1136/JCP.50.1.59>
- Heo, J., Dogra, P., Masi, T. J., Pitt, E. A., de Kruijff, P., Smit, M. J., & Sparer, T. E. (2015). Novel

- Human Cytomegalovirus Viral Chemokines, vCXCL-1s, Display Functional Selectivity for Neutrophil Signaling and Function. *Journal of Immunology (Baltimore, Md. : 1950)*, 195(1), 227–236. <https://doi.org/10.4049/JIMMUNOL.1400291>
- Heo, J., Petheram, S., Demmler, G., Murph, J. R., Adler, S. P., Bale, J., & Sparer, T. E. (2008). Polymorphisms within human cytomegalovirus chemokine (UL146/UL147) and cytokine receptor genes (UL144) are not predictive of sequelae in congenitally infected children. *Virology*, 378(1), 86–96. <https://doi.org/10.1016/J.VIROL.2008.05.002>
- Huang, E. -S, Huong, S. -M, Tegtmeier, G. E., & Alford, C. (1980). CYTOMEGALOVIRUS: GENETIC VARIATION OF VIRAL GENOMES. *Annals of the New York Academy of Sciences*, 354(1), 332–346. <https://doi.org/10.1111/j.1749-6632.1980.tb27976.x>
- Kalser, J., Adler, B., Mach, M., Kropff, B., Puchhammer-Stöckl, E., & Görzer, I. (2017). Differences in Growth Properties among Two Human Cytomegalovirus Glycoprotein O Genotypes. *Frontiers in Microbiology*, 8, 1609. <https://doi.org/10.3389/fmicb.2017.01609>
- Keane, M. P., Arenberg, D. A., Lynch, J. P. 3rd, Whyte, R. I., Iannettoni, M. D., Burdick, M. D., Wilke, C. A., Morris, S. B., Glass, M. C., DiGiovine, B., Kunkel, S. L., & Strieter, R. M. (1997). The CXC chemokines, IL-8 and IP-10, regulate angiogenic activity in idiopathic pulmonary fibrosis. *Journal of Immunology (Baltimore, Md. : 1950)*, 159(3), 1437–1443.
- Keane, M. P., Donnelly, S. C., Belperio, J. A., Goodman, R. B., Dy, M., Burdick, M. D., Fishbein, M. C., & Strieter, R. M. (2002). Imbalance in the expression of CXC chemokines correlates with bronchoalveolar lavage fluid angiogenic activity and procollagen levels in acute respiratory distress syndrome. *Journal of Immunology (Baltimore, Md. : 1950)*, 169(11), 6515–6521. <https://doi.org/10.4049/JIMMUNOL.169.11.6515>
- Klein, M., Schoppel, K., Amvrossiadis, N., & Mach, M. (1999). Strain-Specific Neutralization of Human Cytomegalovirus Isolates by Human Sera. *Journal of Virology*, 73(2), 878. <https://doi.org/10.1128/jvi.73.2.878-886.1999>
- Kraat, Y. J., Hendrix, M. G. R., Geelen, J. L. M. C., Bruggeman, C. A., Wijnen, R. M. H., Peltenburg, H. G., & van Hooff, J. P. (1992). Detection of latent human cytomegalovirus in organ tissue and the correlation with serological status. *Transplant International : Official Journal of the European Society for Organ Transplantation*, 5 Suppl 1, 613–616. [https://doi.org/10.1007/978-3-642-77423-2\\_180](https://doi.org/10.1007/978-3-642-77423-2_180)
- Kurz, S. K., Rapp, M., Steffens, H.-P., Grzimek, N. K. A., Schmalz, S., & Reddehase, M. J. (1999). Focal transcriptional activity of murine cytomegalovirus during latency in the lungs. *Journal of Virology*, 73(1), 482–494. <https://doi.org/10.1128/JVI.73.1.482-494.1999>
- Kurz, S. K., & Reddehase, M. J. (1999). Patchwork Pattern of Transcriptional Reactivation in the Lungs Indicates Sequential Checkpoints in the Transition from Murine Cytomegalovirus Latency to Recurrence. *Journal of Virology*, 73(10), 8612–8622. <https://doi.org/10.1128/JVI.73.10.8612-8622.1999/ASSET/E499D82E-79D0-401F-8736-B1786D388FBF/ASSETS/GRAPHIC/JV1090703006.JPEG>
- Kytö, V., Vuorinen, T., Saukko, P., Lautenschlager, I., Lignitz, E., Saraste, A., & Voipio-Pulkki, L. M. (2005). Cytomegalovirus infection of the heart is common in patients with fatal myocarditis. *Clinical Infectious Diseases*, 40(5), 683–688. <https://doi.org/10.1086/427804/2/40-5-683-FIG002.GIF>
- Lüttichau, H. R. (2010). The Cytomegalovirus UL146 Gene Product vCXCL1 Targets Both CXCR1 and CXCR2 as an Agonist. *The Journal of Biological Chemistry*, 285(12), 9137. <https://doi.org/10.1074/JBC.M109.002774>
- Manuel, O., Åsberg, A., Pang, X., Rollag, H., Emery, V. C., Preiksaitis, J. K., Kumar, D., Pescovitz, M. D., Bignamini, A. A., Hartmann, A., Jardine, A. G., & Humar, A. (2009). Impact of genetic polymorphisms in cytomegalovirus glycoprotein b on outcomes in solid-organ transplant

- recipients with cytomegalovirus disease. *Clinical Infectious Diseases*, 49(8), 1160–1166. <https://doi.org/10.1086/605633>
- Manuel, O., Pang, X. L., Humar, A., Kumar, D., Doucette, K., & Preiksaitis, J. K. (2009). An assessment of donor-to-recipient transmission patterns of human cytomegalovirus by analysis of viral genomic variants. *Journal of Infectious Diseases*, 199(11), 1621–1628. <https://doi.org/10.1086/598952>
- Mattick, C., Dewin, D., Polley, S., Sevilla-Reyes, E., Pignatelli, S., Rawlinson, W., Wilkinson, G., Dal Monte, P., & Gompels, U. A. (2004). Linkage of human cytomegalovirus glycoprotein gO variant groups identified from worldwide clinical isolates with gN genotypes, implications for disease associations and evidence for N-terminal sites of positive selection. *Virology*, 318(2), 582–597. <https://doi.org/10.1016/j.virol.2003.09.036>
- Meyer-König, U., Ebert, K., Schrage, B., Pollak, S., & Hufert, F. T. (1998). Simultaneous infection of healthy people with multiple human cytomegalovirus strains. *Lancet*, 352(9136), 1280–1281. [https://doi.org/10.1016/S0140-6736\(05\)70487-6](https://doi.org/10.1016/S0140-6736(05)70487-6)
- Paraskeva, M., Bailey, M., Levvey, B. J., Griffiths, A. P., Kotsimbos, T. C., Williams, T. P., Snell, G., & Westall, G. (2011). Cytomegalovirus replication within the lung allograft is associated with bronchiolitis obliterans syndrome. *American Journal of Transplantation : Official Journal of the American Society of Transplantation and the American Society of Transplant Surgeons*, 11(10), 2190–2196. <https://doi.org/10.1111/J.1600-6143.2011.03663.X>
- Puchhammer-Stöckl, E., & Görzer, I. (2011). Human cytomegalovirus: An enormous variety of strains and their possible clinical significance in the human host. In *Future Virology* (Vol. 6, Issue 2, pp. 259–271). <https://doi.org/10.2217/fvl.10.87>
- Puchhammer-Stöckl, E., Görzer, I., Zoufaly, A., Jaksch, P., Bauer, C. C., Klepetko, W., & Popow-Kraupp, T. (2006). Emergence of multiple cytomegalovirus strains in blood and lung of lung transplant recipients. *Transplantation*, 81(2), 187–194. <https://doi.org/10.1097/01.tp.0000194858.50812.cb>
- Reddehase, M. J., Balthesen, M., Rapp, M., Jonjić, S., Pavić, I., & Koszinowski, U. H. (1994). The conditions of primary infection define the load of latent viral genome in organs and the risk of recurrent cytomegalovirus disease. *The Journal of Experimental Medicine*, 179(1), 185–193. <https://doi.org/10.1084/JEM.179.1.185>
- Renzette, N., Gibson, L., Bhattacharjee, B., Fisher, D., Schleiss, M. R., Jensen, J. D., & Kowalik, T. F. (2013). Rapid Intrahost Evolution of Human Cytomegalovirus Is Shaped by Demography and Positive Selection. *PLoS Genetics*, 9(9). <https://doi.org/10.1371/journal.pgen.1003735>
- Renzette, N., Gibson, L., Jensen, J. D., & Kowalik, T. F. (2014). Human Cytomegalovirus Intrahost Evolution – A New Avenue for Understanding and Controlling Herpesvirus Infections. *Current Opinion in Virology*, 0, 109. <https://doi.org/10.1016/J.COVIRO.2014.08.001>
- Ribeiro, R. V. P., Ku, T., Wang, A., Pires, L., Ferreira, V. H., Michaelsen, V., Ali, A., Galasso, M., Moshkelgosha, S., Gazzalle, A., Jeppesen, M. G., Rosenkilde, M. M., Liu, M., Singer, L. G., Kumar, D., Keshavjee, S., Sinclair, J., Kledal, T. N., Humar, A., & Cypel, M. (2022). Ex vivo treatment of cytomegalovirus in human donor lungs using a novel chemokine-based immunotoxin. *Journal of Heart and Lung Transplantation*, 41(3), 287–297. <https://doi.org/10.1016/j.healun.2021.10.010>
- Schonian, U., Crombach, M., & Maisch, B. (1993). Assessment of cytomegalovirus DNA and protein expression in patients with myocarditis. *Clinical Immunology and Immunopathology*, 68(2), 229–233. <https://doi.org/10.1006/CLIN.1993.1123>
- Sijmons, S., Thys, K., Mbong Ngwese, M., Van Damme, E., Dvorak, J., Van Loock, M., Li, G., Tachezy, R., Busson, L., Aerssens, J., Van Ranst, M., & Maes, P. (2015). High-throughput analysis of human cytomegalovirus genome diversity highlights the widespread occurrence of

- gene-disrupting mutations and pervasive recombination. *Journal of Virology*, 89(15), 7673–7695. <https://doi.org/10.1128/JVI.00578-15>
- Sowmya, P., & Madhavan, H. N. (2009). Analysis of mixed infections by multiple genotypes of human cytomegalovirus in immunocompromised patients. *Journal of Medical Virology*, 81(5), 861–869. <https://doi.org/10.1002/jmv.21459>
- Suárez, N. M., Blyth, E., Li, K., Ganzenmueller, T., Camiolo, S., Avdic, S., Withers, B., Linnenweber-Held, S., Gwinner, W., Dhingra, A., Heim, A., Schulz, T. F., Gunson, R., Gottlieb, D., Slobedman, B., & Davison, A. J. (2020). Whole-Genome Approach to Assessing Human Cytomegalovirus Dynamics in Transplant Patients Undergoing Antiviral Therapy. *Frontiers in Cellular and Infection Microbiology*, 10. <https://doi.org/10.3389/fcimb.2020.00267>
- Suárez, N. M., Musonda, K. G., Escriva, E., Njenga, M., Agbueze, A., Camiolo, S., Davison, A. J., & Gompels, U. A. (2019). Multiple-Strain Infections of Human Cytomegalovirus With High Genomic Diversity Are Common in Breast Milk From Human Immunodeficiency Virus-Infected Women in Zambia. *The Journal of Infectious Diseases*, 220(5), 792–801. <https://doi.org/10.1093/infdis/jiz209>
- Suárez, N. M., Wilkie, G. S., Hage, E., Camiolo, S., Holton, M., Hughes, J., Maabar, M., Vattipally, S. B., Dhingra, A., Gompels, U. A., Wilkinson, G. W. G., Baldanti, F., Furione, M., Lilleri, D., Arossa, A., Ganzenmueller, T., Gerna, G., Hubáček, P., Schulz, T. F., ... Davison, A. J. (2019). Human cytomegalovirus genomes sequenced directly from clinical material: Variation, multiple-strain infection, recombination, and gene loss. *Journal of Infectious Diseases*, 220(5), 781–791. <https://doi.org/10.1093/infdis/jiz208>
- Subramanian, B., Gao, S., Lercher, M. J., Hu, S., & Chen, W.-H. (2019). Evolview v3: a webserver for visualization, annotation, and management of phylogenetic trees. *Nucleic Acids Research*, 47(W1), W270–W275. <https://doi.org/10.1093/nar/gkz357>
- Sunwen, C., & Norman, D. J. (1988). The influence of donor factors other than serologic status on transmission of cytomegalovirus to transplant recipients. *Transplantation*, 46(1), 89–93. <https://doi.org/10.1097/00007890-198807000-00016>
- Tong, Y., Pang, X. L., Mabilangan, C., & Preiksaitis, J. K. (2017). Determination of the biological form of human cytomegalovirus DNA in the plasma of solid-organ transplant recipients. *Journal of Infectious Diseases*, 215(7), 1094–1101. <https://doi.org/10.1093/infdis/jix069>
- Wang, H. Y., Valencia, S. M., Pfeifer, S. P., Jensen, J. D., Kowalik, T. F., & Permar, S. R. (2021). Common polymorphisms in the glycoproteins of human cytomegalovirus and associated strain-specific immunity. In *Viruses* (Vol. 13, Issue 6). MDPI AG. <https://doi.org/10.3390/v13061106>